Using imine chemistry for post-synthetical covalent chiralization of MOF surfaces

Balázs Álmos Novotny,[†] Sauradeep Majumdar,[†] Andres Ortega-Guerrero,[†] Kevin Maik Jablonka,[†] Elias Moubarak,[†] Natalia Gasilova,[‡] and Berend Smit[*,†]

[†]*Laboratory of Molecular Simulation (LSMO), Institut des Sciences et Ingénierie Chimiques, Valais École Polytechnique Fédérale de Lausanne (EPFL), Rue de l'Industrie 17, CH-1951 Sion, Valais, Switzerland*

[‡]*Mass Spectrometry and Elemental Analysis Platform (MSEAP), Institut des Sciences et Ingénierie Chimiques, Valais École Polytechnique Fédérale de Lausanne (EPFL), Rue de l'Industrie 17, CH-1951 Sion, Valais, Switzerland*

E-mail: berend.smit@epfl.ch

Abstract

Homochiral metal-organic frameworks (MOFs) are exceptional media for heterogenous enantiodifferentation processes. Their rational design, however, is challenging. An available solution for this is moving from constitutive, structure-bearing, homochiral ligands to separating chiral selector and structural roles. This introduces combinatorial modulability, which is the independent change of parts. Such modulability circumvents limitations of designability. Further considerations narrow emphasis to covalent post-synthetic methods. Covalent post-synthetic methods to introduce chirality are reported broadly, yet the diversity of pertaining linkage chemistry is modest. The present work explored the adaptation of imine chemistry for post-synthetic chiralization. A chiral aldehyde and a chiral ketone have been probed, with respective achiral controls,

on two accessible amine-functionalized MOF substrates. Modifying UiO-66 NH_2 with the natural product derived (*R*)-2,2-dimethyl-1,3-dioxolane-4-carboxaldehyde ((*R*)-**1** aldehyde) was found to be the best-performing combination. The modification was shown to be covalent, chiral, and characteristically proceeding through imine formation. A molecular-level inquiry has furthermore revealed that the modification consists of oligomer-rich structures on the surface. *In silico* modeling was shown to predict the localization of the modification correctly. Recent advances in the characterization of MOF color were used to track the imine formation. A strategic approach has yielded a new synthetically facile MOF chiralization method. The modification was shown to result in a surface barrier formation. Thereby, restricted diffusion lengths in the solid phase infer good retention of resolving power in ascending van Deemter régimes in chromatography. This makes the yielding material a promising stationary phase candidate for performant chromatographic enantioseparations.

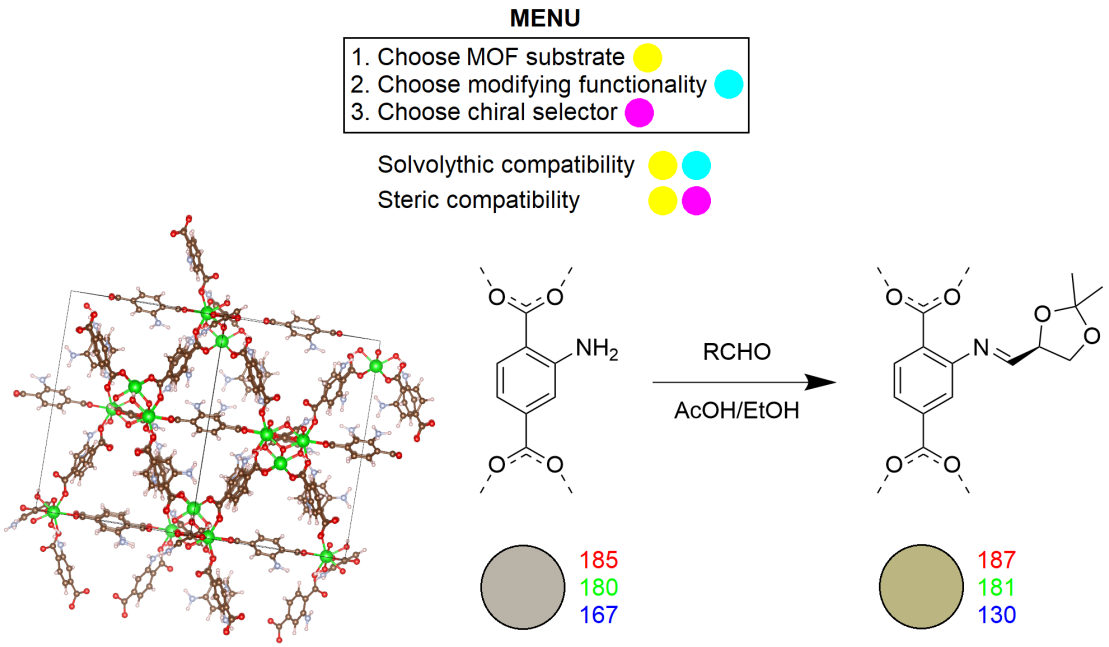

Graphical abstract

Introduction

The first enantioseparation was performed by Pasteur in 1848 when he discovered spontaneous resolution.[1] He obtained large single crystals of a conglomerate forming tartrate salt and sorted them hand based on macroscopic asymmetry. While groundbreaking, the method hardly bore any potential for scalability. However, a successive discovery by Pasteur in 1858 brought about both the purpose and the key to enantioseparation processes.[2] Reporting that microorganisms consume one tartrate enantiomer faster than the other revealed the inherent asymmetry of the metabolome.[3] This foreshadowed the rise of enantioseparation from mere curiosity to a staple process of the pharmaceutical industry, and such inherent asymmetry also yielded the missing tool to perform this.[3]

Enantiomers may only be told apart based on vectorial and not scalar properties. Unfortunately, however, most, if not all, preparative separation techniques differentiate based on scalar properties. This necessitates the association or interaction with an asymmetric media to yield diastereomeric interactions, as diastereomers also differ in their scalar properties.[4–7] The natural feedstock that is the asymmetric metabolome conveniently fills the role of such asymmetric media.[8] Given that an asymmetric pool of products is derivatized from or resolved by a metabolite-based pool of molecules, a minimal number of transformations from thereof are preferred. This benefits both cost and environmental impact via atomic efficiency.

Once the asymmetric media has been used to perform enantiodifferentation, it must be separated from the product. Such a separation from the product is, in most cases, simpler in a heterogeneous system.[9] On a quest to find stable, recyclable, chiral natural product-based solids, metal-organic frameworks (MOFs) fit the description. In addition, by tuning the metal nodes and organic linkers, we can aim to boost the porosity and design materials with enantiospecific steric exclusion.[9–15]

Many such homochiral MOFs, constructed from enantiopure building units, have been reported.[16] These MOFs represent an appreciably large and diverse family of potential enan-

tioseparation media. Interestingly, most of these materials are discovered by serendipity, and only a limited number of materials result from a systematic study to design an enantioseparation media.[17–24] From these studies, we can draw some guidelines, which are all based on the idea to create stereo-selective environments in which only one of the enantiomers preferential adsorbs. However, a strategy to avoid a resource-consuming trial-and-error approach is needed to expand this material family easily.

Refurbishing existing structures is a practical way to avoid trial and error in synthesizing new structures. In these studies, a typical strategy is to start with a "backbone" structure that is indifferent toward introducing an interchangeable enantioselector moiety.[25–27] Various approaches for this are reported, and each has its unique challenges.[25,26] Our contribution begins by outlining the following practical considerations, summarized in Figure 1, which we will use to navigate this field. For example, in the salen family of MOFs, the ligand structure itself allows for modulability, as shown in Figure 1.[16,28–30] Due to less structural constraints, however, "decorating" chiral functionalization strategies are preferred to chiral structural ligands. This functionalization can be done before or after the synthesis.[26] If done before, the enantioselector bearing construct should withstand the conditions of the MOF synthesis. If done after, the MOF should withstand the conditions of the functionalization. These requirements[26] can be referred to as reactive orthogonality. Due to the generally harsher conditions of MOF synthesis, post-synthetic functionalization is often preferred. The functionalization is predominantly introduced either coordinately to the MOF node or covalently to the ligand.[25,26] As enatioseparation process conditions are more likely to introduce competing coordinating agents than to solvolyze covalent bonds, covalent modification is preferred.[3,8]

More chiral selectors or covalent functionalization methods can be added to the toolbox to expand this chemical space. To date, considerably fewer covalent functionalization methods are reported than chiral selectors in the context of MOF. Adding one more covalent functionalization method would yield more new combinations. Beyond these guidelines, a

general criterion that needs to be considered for chiral functionalization is whether the chiral selector can be introduced in the confined space of the pores.[26,27,31] This can be referred to as steric compatibility.

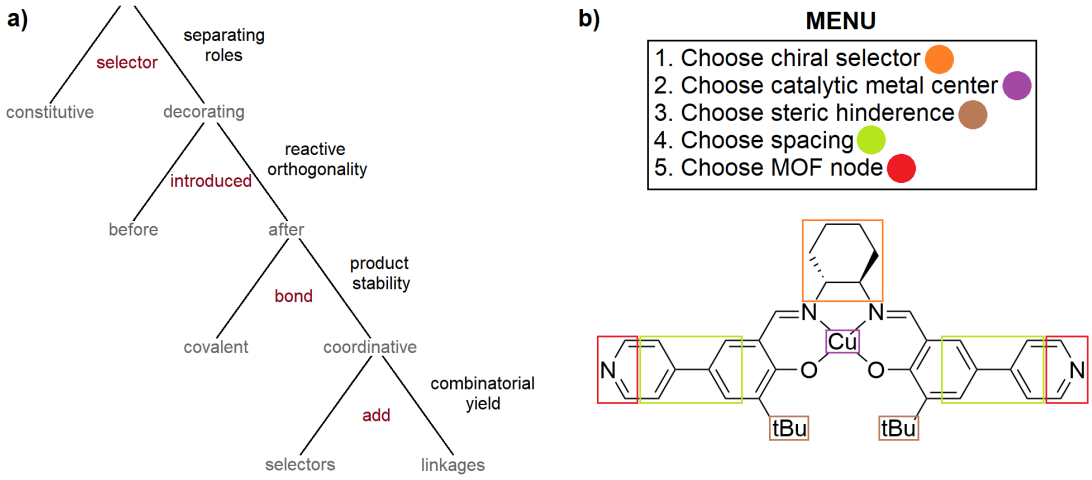

Figure 1: (a) A decision tree summarizing practical considerations for facile material discovery is shown. Maroon text designates decision points, grey text designates options, and black text justifies preference. (b) The modulability of chiral salen ligands is shown with an annotated example.[16] Color coding indicates variable moieties.

This work presents a strategy to navigate and expand the homochiral MOF chemical space. This strategy is based on the observations summarized in the decision tree shown in Figure 1. We show that imine linkage[32] formation, a covalent functionalization, is usable for chiralization. Screening of MOF substrate and modifier pairs has revealed that certain combinations of the reaction conditions necessary for the imine formation can lead to degradation of the MOF. The previously defined reactive orthogonality criterion was found to be limiting viable experimental combinations. The (*R*)-**1** aldehyde modified UiO-66 NH_2 MOF was consequently identified as the flagship combination and was studied further.

To demonstrate that this chiralization was successful, we use a breadth of characterization techniques to thoroughly study the modification from the bulk composition to the molecular level. In addition, *in silico* methods were used to aid our material discovery within chiral functionalization. We use recent advances in MOF color analysis to track imine formation.[33]

Furthermore, we apply pore analysis to study the distribution of the modification. We discuss the previously defined reactive orthogonality and steric compatibility criteria in our experimental context.

Molecular-level inquiry has characterized the statistical oligomerization behavior of the (*R*)-**1** aldehyde modifier. Pore analysis revealed that the modifier may not access the MOF pores, even as a monomer. Results, therefore, suggested a dense enantioselector display on the grain surface. Such implies favorably short diffusion lengths to reach the chiral selectors. This is favorable in chromatographic separation processes.[34]

Synthesis Strategies

Before we describe our systematic synthesis strategy, we first review some of the strategies used in the literature. We thematically highlight the literature on design features that form the foundation of our contribution.

Strategies used in the literature

MOFs from simple chiral metabolites

Inspired by the work of Pasteur, tartric acid has become an archetypal resolving agent.[7] Consequently, some tartrate salt crystal structures may be considered among the earliest homochiral MOF.[16,35,36] Owning to diastereomeric interactions, derivatized tartrates can exhibit enantiospecific coligand incorporation, elevating the transient coordination polymer crystallization itself to the rank of an enantioseparation process.[37] Given how tartrates make excellent ditopic dicarboxylate ligands, fitting the outlined criteria, their numerous stable MOF structures are known.[16] Metalloid-aided enantioduplication is their distinctive feature, allowing for hierarchical framework assembly.[16] Interestingly, monotopic lactate and mandelate building blocks have also found ample use in early studies despite their limited structural role, due to monotopic coordination.[16] Further key chiral metabolite MOF ligands include rigid ditopic camphoric acid,[16,38] alpha substituted ditopic succinates, like aspartate,[16,39,40] and the bulk of the proteinogenic amino acids.[16,39–41] Review literature is ample on homochiral MOF, formed from such carboxylic acid metabolites, and pertaining synthetic derivative ligands.[16]

Natural cyclodextrins can readily be used as MOF ligands, boasting exceptional rigidity, outstanding guest-specific steric exclusion, and extended chiral surfaces.[16,42–45] Their use in enantiodifferentation have been explored.[42,43,45] Given their common edibility, their host-guest interactions are overwhelmingly studied for pharmaceutical formulation.[42–45] Synthetic macrocycle-based homochiral MOF are known,[16,46] some boasting planar and others showing

axial chirality.[46,47] While being exceptional chiral media, their applications are burdened by their challenging synthetic accessibility.[46–48]

The most studied highly synthetic homochiral MOF ligands are the rigid axially chiral binaphthyl family of ligands and the chiral salen type ones.[12,13,16,49–51] Both are mainly studied for enantioselective catalysis,[12,13,49–51] where their exceptional properties as rigid extended catalytic chiral selectors may be credited to permit for some synthetic complexity techno-economically. Examples of further highly synthetic chiral selectors used as MOF ligands are known.[24,52–54] A highlight is the Troeger base, an archetypal centennial chiral selector, with extended rigidity.[53] Despite often improved properties, their slim literature infers associated practical limitations.

Limitations of constitutional homochiral systems

Derivatization of organic metabolite-based chiral MOF ligands may be considered systematic for lactic and amino acid-based systems.[16] Resulting MOFs are, however, structurally distinct. Structural analogues were reported with rigid spacer length[17–19] and sidechain variations,[20–23] only, however, in narrow scope systems. Therefore, the roadmap to diversify the pertaining family of materials is apparently restricted to adding individual materials upon serendipitous discovery. Perspective for rational design is consequently bleak.

Material genomics and computational study of MOF is advancing and can provide design for new structures *in silico*.[55,56] While this may serve as a reassuring clue, no robust methods for translating such results into experimental crystal structures are available.[57–59] Indeed, wishful probing of synthesis conditions of similar known materials remains dominant. Known computational studies on homochiral MOF have been, therefore, primarily focused on characterizing or screening experimentally available systems.[60–65] Computational *de novo* homochiral MOF design has been only reported for functional group variations in narrow scope isostructural systems.[66]

Harnessing orthogonality for chiral MOF design

As pertaining to the MOF structure, the ligands that connect the nodes may be characterized by their size and angular constraints.[67] As long as rigidity, listed constraining features, and coordination chemistry at the node are kept identical, the structural backbone of the MOF may be retained.[31,67] Moving from constitutive chiral linkers to delegating chiral selector and structural pillar purposes to different organic moieties may circumvent the structural aspects of screening difficulties.[26,27] If well-defined angular geometry and rigidity are attainable for constitutive chiral ligands, this strategy is employable without subdelegating roles.[24] Such ligand design, however, is prohibitively demanding from the point of view of organic synthesis.

Having distinct substructures with individual exclusive functions within the material introduces combinatorial modulability, for which prime examples are salen MOF structures.[28–30] Their rigid rod-like interchangeable linkers allow many variations around a common shared motif. Coordination site for the nodes, ligand length, catalytic metal in salen motif, steric accessibility of catalytic metal, and chiral selector may all be chosen orthogonally. Techniques of chiralization via modification aim to achieve the same feat. The avenue of rational design would, therefore, be open.

Achieving such predictable modulability for MOF modifications requires orthogonal reactivities for the chemistry of the structural node and the modification.[26] In the case of pre-synthetic ligand modification, the coordination sites need to be left unaltered, and the modification should withstand the conditions of the MOF synthesis. As for post-synthetic ligand modifications, the MOF is required to be solvolythically stable upon the chiralization step. If coordinative modification is used, changes in the node coordination environment may not interfere with junctions of the structural backbone regardless of approach.

A further limitation of modulability is the steric confinement defined by the MOF pores. Post-synthetic pore penetration of the chiralization reagent may be sterically restricted.[26,27,31] The post-synthetic chiralization process may, furthermore, exhibit self-limiting pore pene-

tration if irreversibly bound modifier blocks reagent transfer, restricting the reaction to the grain shell.[26,31,67] Retention of ample shell porosity for guest molecules is consequential with regards to the nature and performance of prospective sorption-based enantioseparation applications of resulting materials.[34,67] Extendable rod-like ligands yielding isostructural MOF are a good asset to overcome such constraints, while the context of an analogous crystalline system.[68–74]

Pre-synthetic chiralizaiton

If a chiralized analog of a reported achiral structure is made without intermittent isolation of the achiral MOF, the structure is considered pre-synthetically modified.[26] Most common instances of these entail N-acylation of aryl amine bearing ligands, formally with lactic acid[75,76] or proline[68,69,77] moieties. Pre-synthetic introduction of oxazolidinone N-linking Evans auxiliary is also reported.[78,79] Such acylation strategy has also been used for installing a chiral diene.[70] Beyond N-acylation, an instance of O-alkylation with a chiral terpenoid derivative can be mentioned.[71] While modified ligand is prevailingly aminoterephthalic acid,[75–77,79] elongated linear ditopic,[68–70] and tritopic ligands[71,78] are common. The use of alkyne chemistry for linear extension is recurring.[70,71] While chirality to the ligand is introduced leading up to MOF isolation, N-Boc deprotection of prolines[68,69,77] and metalation of diene for catalysis[70] may be undertaken post-synthetically. Pre-synthetic coordinative introduction of chiral agents has also been performed with formally prolinol N-alkylated imidazole, using the same N-Boc protection scheme.[80,81] Defect engineering may, furthermore, be mentioned as coordinative pre-synthetic modifications. Endcapping with monotopic chiral agents bears practical significance, chiralizing surfaces for adsorption-based applications.[82] Despite the ease of synthesis, a less descript product is a disadvantage when it comes to *in silico* interfacing.

Post-synthetic chiralizaiton

Much like for covalent pre-synthetic chiralization, appending the ligands with chiral acylating agents is dominant among post-synthetic strategies. The introduction of proteinogenic amino acids using solid-state peptide chemistry is prevailing.[72,83–89] Account of growing shorter peptides on a MOF solid phase is known.[84] Beyond aminoacyl modifiers, other chiral acylating groups derive from 2-methylbutanoic,[90] mandelic,[86] malic[90] and tartric[86,91] acids. Tartric succinimide modification of aminoterephthalate linker yielding an unprotected chiral diol is, furthermore, known.[91] Apart from carboxylic acid-derived chiral acylating agents, camphorsulfonyl chloride has been used.[86] The MOF taking the role of the acylating agent has also been reported for chiralization, by trapping diol-bearing sialic acid with boronic acid presenting a solid phase, with favorable selectivity under mild conditions.[92] All of these examples boast natural stock-derived chiralizing agents. Post-synthetic covalent chiralization is less prevalent via alkylation, reported with a chiral epoxide.[86] The workhorse of biorthogonal chemistry, click chemistry, has been reported to append MOF using prolinol-derived azide reagent.[73,93] The steric exigence of the triazole click linkage may be credited to the limited literature on this approach. Successful chromatographic enantioseparation with covalently chiralized solid phases is reported in multiple instances for surveyed strategies.[85–87]

Coordinative modification is also prevailing in post-synthetic chiralization literature. Unmodified proteinogenic amino acids are the protagonist of this subfield, as well.[94–100] Tartric acid,[100–102] lactic acid,[98] and ibuprophen[98] are furthermore employed. Coordination is shown to be commonly formed by the carboxylate. Proline acylated aminopyridine[103] and (1*R*,2*R*)-1,2-diphenylethylenediamine,[104] however, have been reported to introduce chirality via N-coordination of structural metal cations in nodes. Coordinative defect engineering has also been reported post-synthetically, relying on ligand exchange in this instance, with linear Salen-type chiral dicarboxylates.[105,106]

Beyond covalent and coordinative post-synthetic chiralization, examples using ion exchange and guest molecule trapping are known. Dimethylammonium counter ions in charged

frameworks were reported to be replaced with N-benzylquininium, a natural chiral stock-derived selector cation.[74] As for trapping, Salen-type chiral guest molecules were shown to be immobilized in pores by in situ acylation, which sterically prohibits further displacement of such catalytically active guests.[107]

Strategies used in this work

Given that harsh reaction conditions of MOF syntheses are feared to be prone to result in solvolysis and racemization, enriching post-synthetic chiralization is preferentially explored in this work. Considering how such modification chemistries are so far found to be dominated by a couple of highly analogous methods, diversification of the modes of chiralization merits attention. In this work, we pursue a novel modification chemistry. Surveying covalent-organic post-synthetic modification strategies, yet outside the scope of chiralization, reveals two pertinent prospective ligations, phosgene and imine chemistries. Further, more marginal examples are cycloadditions beyond click chemistry,[108] and using epoxidized MOF as alkylating matrix.[109]

A noteworthy take on acylations in the present context entails using isocyanate and isothiocyanate chemistry.[110] Phosgene and thiophosgene may produce such potent acylating groups from amino groups on either the substrate[111–113] or the modifying agent.[90,114–117] This versatile system may yield activated crystalline substrates that readily covalently trap nucleophilic agents in pores. Highly pronounced safety concerns pertaining to gaseous carcinogens, and the necessity of strictly anhydrous and otherwise nucleophile-free systems are, however, deterrents for further exploration.

Another covalent modification technique is imine formation.[32] Just like with phosgene chemistry, achiral exploitation of this post-synthetic covalent appending technique has been used with interchangeable positioning of reactive functionalities. Aldehyde-bearing substrates, both a dicarboxylate ligand[118] and ZIF-90,[119] have been submitted to this reaction. As for amine-bearing substrates, they have been reportedly modified with salicylic

aldehyde broadly,[120–125] with aldehyde bearing pyridine derivatives,[126,127] with aldehyde bearing imidazole,[128,129] with 8-hydroxy-2-quinolinecarboxaldehyde,[130] with aldehyde bearing pyrene,[131] with 2,3,4-trihydroxybenzaldehyde,[132] and with formaldehyde.[133] Many of such amine-bearing substrate modifications have culminated in post-synthetic metalation, thereby introducing new coordination sites.[120–123,125–128,130] Imine functionalization with a ketone was reported in the context of a direct reaction with an acetylacetone metal complex, yielding covalent modification and post-synthetic metalation in a single step.[134] Interestingly, achiral modification via imine formation has also been performed on otherwise amino acyl chiralized MOF.[72,88] Just like phosgene chemistry, imine formation was not reported for MOF chiralization to date, to our knowledge. Much unlike phosgene chemistry, however, this requires lesser exigence, linking amino groups with oxo compounds in warm ethanolous media. Application of this reaction for chiralization was therefore undertaken in this study.

Considering the poor stability of aldehydes and the modest accessibility of such substrates, the MOF was assigned to bear the amino precursor of the Schiff-base linkage. Given the ample literature on and good precursor availability for aminoterephthalate MOF in general,[135,136] and especially for aminoterephthalate analogs of MIL-125[137] and UiO-66,[138] the latter two were chosen. As for the oxo compounds, simple archetypal chiral natural products were targeted. Glyceraldehyde, the simplest aldose, was chosen in the form of its acetonide-protected derivative. Such may be conveniently derived via the periodate cleavage of mannitol diacetonide synthetically.[139,140] As for the ketone, rigid, configurationally locked, sterically confined camphor was chosen.

Probing the resulting combinatorial space was intended to assess the stated reactivity limitations, substrate stability, steric confinement, and reagent penetration. Acetaldehyde and acetone were chosen as positive controls for reactivity, more permissive on steric and diffusion rates, considering their size. Acetone is the smallest ketone, while acetaldehyde is the second to smallest aldehyde to formaldehyde, the latter avoided due to polymerization and excessive toxicity.

The primary question is whether and when compositional change can be achieved while leaving the backbone of the MOF substrate structurally and solvolythically intact. In addition, we would like to confirm that modification is indeed a covalent chiralization via imine formation. And, finally, investigate what sorption-based separation such modification may allow based on the resulting grain and pore structures.

The initial mode of inquiry entails characterization techniques of the bulk composition of the product. Apart from the key techniques of thermogravimetric analysis, TGA, and elemental analysis, yields may help to infer compositional change. Another essential mode of inquiry concerns chromophore-based techniques, inherent to the underlying imine chemistry. In the visual spectrum, changes in MOF color and reaction solution color are indicative and may be further supplemented by Fourier-transform infrared spectroscopy (FT-IR). Chromophore formation, furthermore, allows direct inquiry into enantiomeric excess via circular dichroism, CD. Inquiry concerning the crystalline structure of the framework substrates entails powder X-ray diffraction, PXRD, and experiments. Molecular level structure and composition may be elucidated by nuclear magnetic resonance, NMR, and high-resolution accurate mass electrospray ionization mass spectrometry, HRAM-ESI-MS, based techniques, with the aid of solution state model experiments and digestions. Experimental modes of inquiry may be supplemented by *in silico* modelling, entailing the assessment of the sterics of target modifications, and the pore analysis of the pertaining systems.

Methods

Materials

Starting MOF substrates MIL-125 NH_2[141] and UiO-66 NH_2[142] were previously synthesized according to the referenced procedures. For modification experiments, (*R*)-2,2-dimethyl-1,3-dioxolane-4-carboxaldehyde ((*R*)-**1** aldehyde) (50% in methylene chloride, 95%, 5 g) was purchased from Chemie Brunschwig AG, D-camphor (95%) from Fluorochem, acetaldehyde

(puriss. p.a., anhydrous, 99.5% GC) from Sigma-Aldrich, acetone (p.a.) from Sigma-Aldrich, acetic acid (glacial, p.a.) from Merck Millipore, trifluoroacetic acid (99%) from SIAL, ethanol (p.a., absolute) from Fisher Chemical, and 2-aminoterephthalic acid (99%) from Sigma-Aldrich. For model experiments, deuterated methylene chloride (99.8% D) was purchased from Cambridge Isotope Laboratories, deuterated methanol (99.8% D, glass ampoule) from Chemie Brunschwig AG, dimethyl 2-aminoterephthalate (97%) from Fluorochem, and dichloromethane (anhydrous, 99.8%, contains 40-150 ppm amylene as stabilizer) from Sigma-Aldrich. For digestion experiments, cesium carbonate (99.9000% trace metals basis) was purchased from Sigma-Aldrich, and ammonium bicarbonate (99%) from SIAL. All chemicals were used as received, without further purification. The water for all experiments, Milli−Q purity, was obtained from Integral 5, Elix Technology machine by Merck Millipore. Compressed, on tap, nitrogen gas stemmed from liquid nitrogen (≥99.9%), supplied by Carbagas AG.

Methods for MOF modification

Each sample was treated in a plastic-capped 12 mL glass vial. For positive and negative controls, 10 mg of respective MIL-125 NH_2 or UiO-66 NH_2 MOF substrate was used. As for attempted chiralization, a 20 mg sample per vial was used. To each vial, 5 mL ethanol and 150 µL of glacial acetic acid were added. No modifying reagent was added for negative controls, while for positive controls, 300 µL of acetaldehyde, or 400 µL of acetone was added per vial. As for chiralization 300 mg of (*R*)-**1** aldehyde 50% solution, or 400 mg of D-camphor was added. For reaction with D-camphor, a free control, containing 30 mg of 2-aminoterephthalic acid instead of the MOF was included. Ease of handling was reflected in weighing accuracy for reagents. All vials were capped thoroughly with parafilm under cap, and were then heated to 80 °C for 24 h. All samples containing D-camphor were supplemented with 150 µL of TFA when cold, following initial treatment, and were then recapped and returned for a second treatment for 24 h, at 100 °C this time. All thermal treatments were performed in a

Carbolite programmable oven, inside a ventilated fume hood, model experiments included. Uniformly, heating rates of 2.0 °C min^{-1} and cooling rates of 0.2 °C min^{-1} were used, with a forced ramp not guaranteed upon cooling, for model experiments alike. Solids were washed once with 8 mL of ethanol per vial for positive and negative controls. When a chiral modifying agent was present, treated solids were washed with four times 10 mL of ethanol each, over the course of 3 days. Solids were aspirated upon washing and were collected by gravitational settling in original reaction vials, with supernatants removed by pipette. A minimum of 4-day ambient drying was ensured for each sample before analyses.

Methods for homogenous model experiments

Model 1

Objective: Reproducing reaction in deuterated medium To an NMR tube, 15 mg of dimethyl 2-aminoterephthalate was added. A 750 µL ampoule of D4-methanol was taken with a glass pipette and flushed over (*R*)-**1** aldehyde 50% viscous solution, then transferred into the NMR tube. The capped NMR sample was treated at 70 °C for 20 h. Yielding condensed residue was redissolved in an identical, matching amount of fresh solvent. The obtained clear solution was stored at 4 °C.

Model 2

Objective: Reproducing reaction under deoligomerization favoring conditions To a 12 mL glass vial, 500 mg of 2-aminoterephthalic acid and 8 mL of ethanol were added. A 500 µL of methylene chloride was taken with a glass pipette and flushed over (*R*)-**1** aldehyde 50% viscous solution cold, then transferred into the vial. The plastic cap was fit tight without parafilm, and the mixture was treated at 80 °C for 24 h. A sample of the resulting clear solution was taken using a glass pipette without disturbing the settled-out solid and stored at 4 °C.

Model 3

Objective: Reproducing reaction under the conditions of solid-phase treatment To a 12 mL glass vial, 20 mg of dimethyl 2-aminoterephthalate, 5 mL of ethanol, and 150 µL of glacial acetic acid were added. A 300 µL of (*R*)-**1** aldehyde 50% was transferred into the vial. The plastic cap was fit tight using parafilm, and the mixture was treated at 80 °C for 24 h. A sample of the clear solution was drawn using a glass pipette, and stored at 4 °C.

Methods for digestion experiments

Digestion method 1

Objective: Solubilization in nucleophilic ammonia-free aqueous medium Solid analyte consisted of either 10 mg of treated MOF or a 400 µL residue of Model 2 solution obtained by drying with on-tap nitrogen gas flow. For each sample, digestion solutions were prepared by dissolving 100 mg of cesium carbonate in 650 µL of water in a glass vial. The digestion media were pipetted to respective analytes, and samples were mixed gently by tilting in capped glass vials. After some minutes, another 350 µL fresh digestion solution of identical composition was pipetted to each sample. Gentle mixing continued for another 0.5 h, and a minimum total digestion time of 24 h elapsed before analyses. Pertaining drying and digestion took place at ambient temperature. The completion of digestion was verified before analyses by checking the solution clarity and for lack of sedimentation.

Digestion method 2

Objective: Solubilization in pH-neutral aqueous medium Treated MOF analyte, 5 mg, was suspended in 700 µL of water for easy handling by pipette. A near-saturated aqueous ammonium bicarbonate solution was freshly prepared from the solid salt. Yielding liquids were mixed in various ratios and were vigorously aspirated for up to 10 min. The remaining solids were collected by 1 min of centrifugation at 2374 RCF in GmCLab Gilson Capsulfuge

PMC-880, rendering digestion partial. Clear supernatants were removed by pipette and were subjected to immediate measurements. The procedure was performed at ambient temperature using plastic labware.

Characterization techniques

Weighing was done on a Mettler Toledo XP205 balance.

Thermogravimetric analysis (TGA) traces were obtained on NETZSCH TGA209 F1 Libra instrument. A 10 mL min^{-1} airflow and a 20 mL min^{-1} protective nitrogen gas flow were employed. Samples were measured from ambient temperature to 700 °C, using a ramp speed of 5 °C/min. Alumina crucibles, 85 µL, NETZSCH GB399972, were used without lid, filled up to 15 mg of solid analyte, and calcined before use.

Elemental analyses were performed on an Elementar Unicube instrument, employing an 1150 °C furnace and direct Temperature Programmed desorption. Samples were measured in triplicate.

Powder X-ray diffractograms (PXRD) were accumulated on Bruker D8 Advance diffractometers, from 1.000° to 60.145° 2θ angle, using 2883 times 0.021° steps, 0.50 s per step. Measured at 25 °C, with 5.00 min^{-1} sample rotation. Generator with settings 40.0 kV, 40.0 mA, with Cu anode, and 0.2 µm Ni low $\kappa\beta$ filter used. The detector was LYNXEYE XE, 2.948° opening, ranges between 0.202 V and 0.232 V, with fixed slits, with both primary and secondary Soller slit at 2.500° limit. Low background Si sample holders from Bruker were used with 51.5 mm and 24.5 mm respective support and Si diameters.

Photography was performed in an illuminated ML-4030 Led Maxi Light Box with Datacolor Spyder CHECKR 24 color correction card, using the main camera of a Techno Camon 17 cell phone. White point color correction was done according to the reported procedure.[33]

Fourier-transform infrared spectroscopy (FT-IR) was performed on Spectrum Two™ from Perkin Elmer, with background subtractions, using direct measurement from treated MOF powders.

All nuclear magnetic resonance (NMR) experiments were performed with a Bruker (AV-III) spectrometer equipped with a 5 mm BBO probe head capable of producing magnetic field pulse gradients in the z-direction of 54 G·cm^{-1}. Frequencies are 400.13 MHz for ^{1}H NMR and 100.62 MHz for ^{13}C NMR experiments. Standard Bruker parameters set were used for magnitude mode COSY (cosygpppqf), edited HSQC (hsqcedetgpissp2.3), and HMBC (hmbcgplpndqf). The Bruker DOSY pulse sequence (ledbpgp2s) was used to measure diffusion coefficients. The DOSY diffusion time interval (d20) and gradient pulse length (p30) were set at 1000 µs and 60 ms, respectively, with a recycle delay (d1) of 3 s. Each 1D free induction decay had 4K complex points with 32 scans averaged. The diffusion gradients were ramped from 2% to 98% at linear increments to generate 32 increments in the diffusion dimension. All experiments were performed at 298 K temperature, each taking about 50 min. DOSY NMR data processing was performed using MestreNova software.

The high-resolution accurate mass electrospray ionization mass spectra (HRAM-ESI-MS) were accumulated using an automated chip-based nanoelectrospray device (Triversa Nanomate, Advion, Ithaca, U.S.A.) coupled to Orbitrap Exploris 240 FT-MS instrument. Following calibration, samples were measured using direct injection in acetonitrile dilution in negative mode, and 0.1 V/V% formic acid containing acetonitrile dilution for positive mode. Mass spectra accumulated from m/z of 100 to m/z of 1000. The tandem mass spectrometric (ESI-MS/MS) experiment was performed in the same setup with HCD fragmentation from m/z of 50 to m/z of 520. An internal calibration option EASY-IC was activated to achieve the highest possible mass accuracy (< 1 ppm).

Circular dichroism (CD) spectra were obtained on a Chirascan V100 spectropolarimeter, with samples being held in a quart cuvette of 1 mm path length. Necessary dilutions were performed with respective neat solvents.

Results and discussion

Results and discussion were organized according to three main approaches. Analyses of the bulk composition will reveal the quantitative aspects of the modification attempts, followed by the key reactivity trends. The molecular-level inquiry will line up evidence from organic chemistry characterization techniques. Computational structural modeling will reveal the sterics of the system to help find a comprehensive interpretation of these two groups of experimental results.

Compositional change in light of solvothermal stability of substrate

Here, we use a combination of experimental techniques to show how the bulk composition of our samples evolves upon attempted modification. In particular, we use TGA to probe the thermolabile mass fractions specifically. Elemental analysis is used as a complementary technique to better ascertain the nature of mass incorporations. Solution color and yield are further considered as indicators for solvolythic substrate dissolution. In turn, PXRD is used to probe the crystallinity of solid isolates.

TGA: bulk modification

Accumulating thermogravimetric traces in air-exposed open crucibles up to 700 °C allows for the quantitative removal of organic components. Supposing complete sample calcination, the found composition can be referenced to stoichiometry by normalizing thermogravimetric traces on the residue mass. A decay curve, revealing the relative thermolabile mass, is thereby obtained. Subtracting the normalized traces of the modifying agent free control from that of the attempted modification of interest reveals the decay of thermolabile relative mass-increase creditable to the modifier. Expected thermolabile mass ratios for all traces, assuming full conversion, may be found, and realized conversion may be inferred therefrom.

All thermogravimetric traces of concern have reached a thermostable plateau, confirming

that the posited quantitative calcination criterion was met. More so than the UiO-66 NH_2 modifier free control, the MIL-125 NH_2 one fell short of expectations on thermolabile relative mass, prompting solvolysis concerns. Harsher conditions for reacting the D-camphor badly reduced the thermolabile relative mass for MIL-125 NH_2, demonstrating solvolythic ligand leaching to be dominant. While disconcerted thermal events impede clear interpretation for the analogous UiO-66 NH_2 probe, the lack of such decrease makes a strong case for the superior stability of this substrate. Probes with acetaldehyde led to a relative organic mass incorporation increase that exceeded expectations. Such may be credited to interface polarity shift improving interactions with solvent molecules. The temperature profile, showing a considerable slope in low-temperature régimes, is consistent with such. Relative increases for probes with the (*R*)-**1** aldehyde fit within expectations, yet the low-temperature sloping of their profiles draws caution for deeper interpretation. Probes with the acetone allude to incorporation with profiles reflecting thermal stability despite expectations of a poorer extent of covalent attachment. In Figure 2, a comparison of normalized thermogravimetric traces is shown.

A potential caveat to the initially outlined facile assessment may be the solvolythic degradation of MOF, leading to a simultaneous decrease of thermolabile relative mass via organic ligand leaching. Assuming that solvolythic degradation under otherwise identical reaction conditions is largely independent of the modifier present, such is accounted for by subtracting the traces of controls. Adding a further layer of complexity is the expected presence of physisorbed solvent for controls and attempted modifications. The thermolabile relative mass decay profile may be telling when it comes to discerning physisorbed solvents from covalent modifications. While the former is expected to be gradually released at lower temperatures, the latter is expected to be retained until the oxidative collapse of the framework. Despite such elaborations, the method has key limitations. The physisorbed solvent retention may improve considerably if the modification results in pore closure in the grain shell. Interface modification may also greatly impact physisorbed solvent uptake and retention. Further-

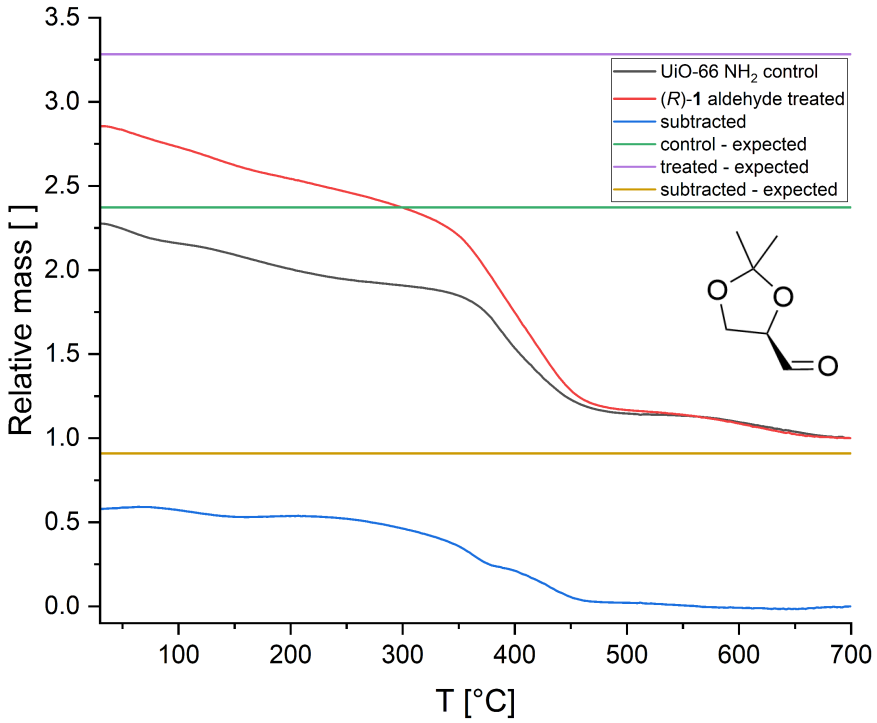

Figure 2: The thermogravimetric traces normalized on the calcined residues. Respective traces for treated substrate, control, and their difference are shown. Corresponding expected thermolabile relative masses, based on the stoichiometry of full conversion, are overlaid. Plot pertains to UiO-66 NH_2 substrate treated with oxo compound (*R*)-**1** aldehyde.

more, as the method only infers the strength of the interaction, incorporating the extended modifier as a guest may not be discernible from covalent binding.

These findings stress the limitations in the compatibility of the surveyed chemical space. The present study, in consequence, pursued prioritizing the substrate with better solvolythic stability and the oxo modifier with better reactivity. The MIL-125 NH_2 D-camphor system was thus excluded from further inquiry, and the UiO-66 NH_2 (*R*)-**1** aldehyde one gained focus. In light of stated method limitations, apparent modifier incorporations were not deemed conclusive before successive experiments.

Elemental analysis: bulk modification

Elemental analysis adds further detail concerning the composition of surveyed solids. The MIL-125 NH_2 system was found to retain DMF from the solvothermal synthesis, based on its N content, while for UiO-66 NH_2, the results were in line with theoretical ligand N contribution. The three surveyed attempted chiralizations have all resulted in a carbon-dominant increase in organic content. Such an increase was, however, consistently falling short of the theoretical values for uniform modifications. Unlike TGA, however, herein insight is only provided for the room temperature isolates, leaving no room to delimit contribution from physisorbed species. Contrasting the modest number of channels in CHN analysis with the diversity of species the isolates have encountered from the MOF syntheses, interpretation may only be holistic in nature. The N channel boasts specificity, as it may only indicate DMF retained from the syntheses, apart from the aminoterephthalate ligand. As such, if the presence of DMF is not revealed in controls, the N content of the ligand may serve as an internal standard to reference CH content. As for the CH channels, degrees of unsaturation for incorporated species may be inferred. Such serves as a basis for holistic analysis, associating higher H content with solvent-rich and higher C content with modifier-rich isolates. Metal content ascertained via TGA may be used to delimit unaccounted mass fraction and assign it to O content. Such analysis was, however, eluded due to inherent uncertainty re-

garding elemental exclusivity and methodological coherence. In summary, findings support the success of modifier incorporation into recovered solids and demonstrate that quantitative appending of structural ligands, however, may not have been obtained.

Solution color: partial MOF dissolution

The orangish color shift associated with the expected imine chromophore is an exceptional analytical asset, as it may be evaluated promptly without instrumentation. For UiO-66 NH_2, microcrystalline substrate settled slowly from solution. Nevertheless, the solution did not retain an orange taint upon eventual clearing. For MIL-125 NH_2, however, the orange coloration of particulate-free reaction mixtures was highly evident. Solution color may not only reveal the presence but also the localization of the product. Released MOF ligands in solution have an advantage for imine formation over bounded ones due to steric accessibility. Therefore, the reaction solution's orangish taint is a robust indicator for ligand leaching. Earlier findings on solvolythic substrate stability were confirmed by the presence of the iminie chromophore, and thereby the presence of the leached ligand, in reaction mixtures. The UiO-66 NH_2 substrate was determined to perform considerably better with regard to ligand retention under relevant reaction conditions.

Yield: partial MOF dissolution

While the aforementioned analyses were discussed to reveal solvolythic substrate degradation, mass recovery may be regarded as the most direct indicator. For UiO-66 NH_2, isolated solids measured up, at minimum, to the mass of the starting substrate. However, for MIL-125 NH_2, solid masses were halved when subjected to modification conditions and decimated under the harsher conditions used with D-camphor. Given how desired modifications are incorporations, the mass of the isolated solid may unequivocally reveal substrate solubilization if it is inferior to the starting amount. Such observations have strongly confirmed and quantitatively nuanced the already established trends in solvolythic substrate stability.

PXRD: retention of backbone crystallinity

The crystallinity of the solid isolates was probed by PXRD. For all hereby evaluated chiralization attempts, the PXRD patterns closely matched that of respective starting substrates. In Figure 3, the matching of the diffractograms is demonstrated. Reflections in PXRD patterns correspond to distances inherent to respective sets of parallel planes. The size of the electron shell of concerned atoms determines the intensity of such reflections. Consequently, in the present study, PXRD primarily reveals the relative position of metal nodes. This outcome has thus revealed that the structural backbone of the framework, spacing, and relative angular position of the nodes have been largely left intact in the recovered solids. Whatever modification may have thereby been performed can be, therefore, considered orthogonal to the backbone structure.

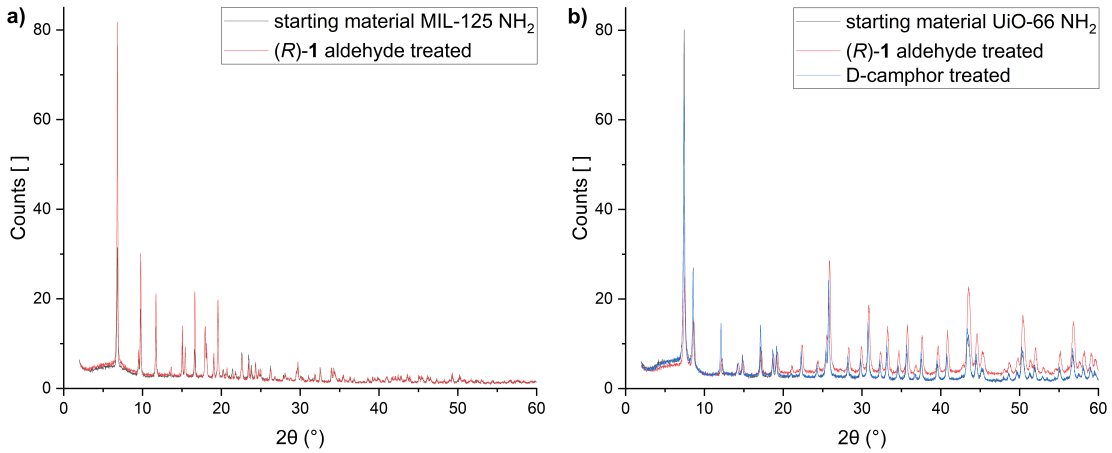

Figure 3: Pattern retention of the powder X-ray diffractograms for MIL-125 NH_2 (a), and UiO-66 NH_2 (b) substrates. The plot overlays diffractograms of the untreated and treated substrates.

Covalent and chiral nature of modification

Here, we use a combination of experimental techniques to study how the molecular-level composition of the samples evolves upon attempted modification. We assess color change and use FT-IR spectroscopy to probe for the formation of the imine chromophore. We use

NMR to study components of solution state model systems. Importantly, HRAM-ESI-MS is applied to elucidate the composition and formation route of solubilized product mixtures. Enantiomeric excess is, in turn, probed for using CD spectroscopy.

Color change: covalent modification in shell

The characteristic color of the imine chromophore may be exploited as an immediate facile indicator not only in solution but also on the treated MOF. A pronounced color shift was observed in all cases for attempted modifications involving aldehydes. For MIL-125 NH_2, from ripe yellow to a dark orangish-brown color, while for UiO-66 NH_2, from light cream to a greyish dark brown color. However, no visually unequivocally interpretable color shift was seen with acetone. As with the D-camphor, under the harsher conditions, the color shift for the MIL-125 NH_2 was pronounced, while for UiO-66 NH_2 it was less apparent. Photographs of the starting materials and of isolates from attempted chiralizations were taken where yield was sufficient for the latter. Comparison of calibrated colors has, nevertheless, revealed a shift to be statistically significant in all photographically studied cases. In Figure 4, the calibrated colors are shown. The outcome gives strong direct evidence that all aldehyde treatments have resulted in imine formation in the solid phase. Bleak evidence for the same in the case of ketone treatments further discourages pursuing that half of the chemical space. While a direct indicator of the covalent modification on the solid, isolate color does not reveal the radial distribution of the modification.

FT-IR: covalent modification in shell

The FT-IR spectra reveal the underlying functional group chemistry, much like the appearance of the visually observable chromophore. Spectral evidence of covalent modification was found, where imine formation was expected. While this spectroscopic method is considerably superior to photography in spectral resolution and breadth, it shares similar limitations regarding grain shell penetration. These findings, therefore, only back color-based evidence

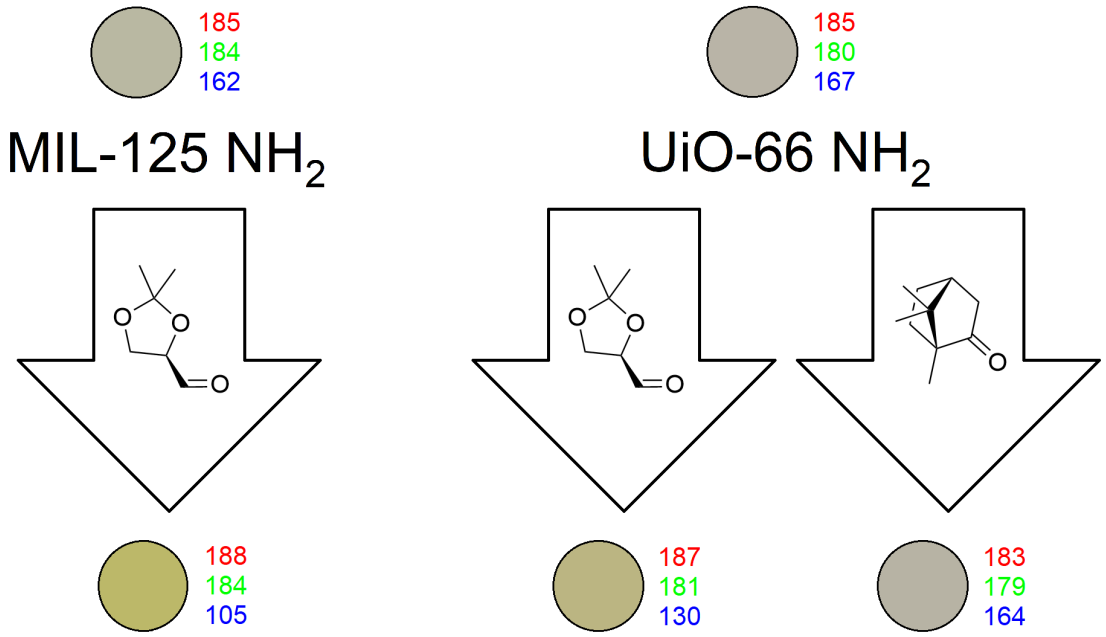

Figure 4: The white point corrected colors of untreated and treated substrates are compared to the probe for the orangish color shift attributable to the imine chromophore. A representative average of each color is sampled and described with the corresponding RGB code. Substrates (top), and chiral modifiers (arrows) are indicated.

of modification on the surface.

NMR: mixture formation

Analyses by NMR are a powerful tool to ascertain the molecular structure of a species of interest in solution; applicability of such in present work is, however, indirect. Model 1 experiment was constructed to elucidate characteristic and distinguishably unique chemical shifts of the target product. Model 1 experiment was tracked by one-dimensional NMR techniques, and yielding matter was studied by two-dimensional NMR techniques. Molecular motifs of reagents could be assigned to distinguishable chemical shift ranges. A considerable number of resolvable signals within all of these ranges were seen. Findings suggest that a large number of distinct species are formed, presumably in a statistical matter, owing to the versatility of aldehyde chemistry. A multitude of signals in each chemical shift range suggests that all introduced reagent moieties are incorporated into more than one underlying species.

Considering sample size and purity requirements, applicability of post-digestion NMR was deemed poor, in light of this outcome. While solid-state NMR could even allow for direct study of modified MOF, it would require a more robust *ab initio* knowledge of the system. Therefore, NMR techniques were deemed prohibitively challenged for further inquiry in the present study.

HRAM-ESI-MS: dominant ligand modifications

Analysis by HRAM-ESI-MS is considered an apt tool for characterizing mixtures, especially if statistical product formation is involved. Key probed systems were chosen to be Model 2, and Digestion method 1 applied to both Model 2 and the (*R*)-**1** aldehyde treated UiO-66 NH_2 product. The ten most intense signals were analyzed with primary, laxed, chemical bias, while the one hundred most intense signals were cross-referenced with found masses conforming to a statistical set. This set was generated by acetonide hydrolysis, acetal, and oxomethylene chain formation, with hemiaminal adducts on imine permitted as applicable.

Alongside expected condensed imines, hemiaminals were found to be common in all mixtures. The ethanolous Model 2 solution was richer in dimeric adducts of modifier, tethered predominantly via an oxomethylene backbone. The corresponding aqueous mock-digestion revealed a shift to deoligomerization, upon exposure to a new medium. Deacetonidation was, in turn, found to be most prevalent in the MOF digestion product. The latter also had a distinctive prevalence of N-formylated substrate, when analyzed without the constraints of the set. In Figure 5, representative species recovered directly from MOF digestion are shown.

Model 2 was chosen due to identical process conditions and an excess of unmodified ligands presumably representing the expected matrix. This presumption was based on found partial conversion, and expectations of hindered modifier penetration. Digestion of zirconium MOF using aqueous carbonate solutions was inspired by literature.[143] Owning to the competitive coordination of carbonates, such allows for framework solubilization in hydrolytically

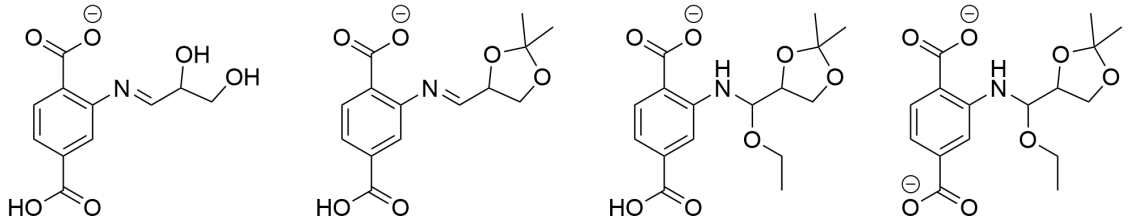

Figure 5: The ions, conforming to the constrained statistical product set, that have been directly detected among the one hundred strongest ESI-MS signals of the Digestion 1 solution of the (*R*)-**1** aldehyde treated UiO-66 NH_2 substrate.

milder pH régimes. Digestion method 1 was preferred as Digestion method 2 was feared to release nucleophilic ammonia. Cesium cations were chosen to moderate matrix ionizability.

Mass accuracy has allowed for elucidation of the elemental composition upon imposing primary chemical constraints. In light of stellar sensitivity, caution is advisable as external contaminants may not conform to primary constraints. Consequently, interpretation of the most intense signals was warranted. As for signal intensity, the ionizability of species varies, although such may be presumed to be moderated by chemical similarity. In the present context, however, expected coordinative oligoether interactions with alkaline cations drew further caution.[144] Analysis, therefore, required reserve with regards to prevalence to intensity correlativity. Positing which reactions govern presumed statistical product formation introduced further chemical bias. Representativeness of the model, therefore, needed to be validated.

The N-formylated substrate, found in the MOF digestion, may be assigned to transacylation from DMF during MOF synthesis. This deactivation of the functionalization is a further limitation to the desired orthogonality in reactivities. However, the extent of the phenomena was assessed to be moderately consequential. Findings have validated the chemical model that arose from a preconception regarding dominant reaction types, as removing such bias reflected a coherent interpretation. Furthermore, the prevalence of the underlying reaction types was correlated with reaction conditions of interest. Importantly, analysis of

the digestion sample gave direct evidence that the target species, the formal imine adduct, is characteristic of the modification on the MOF.

CD: retention of enantiomeric excess

Measuring solution CD was considered to be applicable, given that species of interest can be solubilized. Differential absorption of circularly polarized light by an asymmetric pool of chromophore-bearing molecules thereby becomes assessable. The presence of a visually detectable chromophore was confirmed by absorbance for all three ethanolous model solutions. Cesium carbonate containing Digestion method 1 medium has consistently solubilized chromophores, while incomplete solubilization with ammonium carbonate containing Digestion method 2 yielded a low chromophore concentration. The presence of enantiomeric excess has been clearly ascertained in Model 1 and Model 3 solutions, but not for Model 2. Indication of enantiomeric excess, however, has not been deemed significant for any of the MOF and mock digestion experiments.

However, a key limitation of the method was the required proximity of the chromophore to the chiral moiety, necessitating a positive control to validate the method. Furthermore, for successful measurement, absorbance needs to be fine-tuned with dilutions to optimize the signal-to-noise ratio, as both over-dilution and poor transmission may be limiting. High absorbance backgrounds, therefore, may also have impeded the detection of enantiomeric excess. Detection of enantiomeric excess in the case of Model 1 and Model 3 experiments has demonstrated the sufficient proximity of the chromophore to the chiral moiety. Given how Model 3 reaction conditions tightly match that of the MOF modification, the pertaining environment allowed for the retention of enantiomeric excess. Such can be interpreted as indirect evidence that modification of MOF does introduce an enantiomeric excess bearing pool of appending auxiliaries. As enantiomeric excess was not clearly detected in any digestion experiments, direct evidence of chiralization was not obtained. Reflecting on the negative CD outcome of the Model 2 solution, the presumed culprit is a high absorbance background

attributable to a large excess of the achiral unmodified ligand. Modest conversions would translate to such excess when modified MOFs are digested. Carbonate species-rich media may, furthermore, worsen background absorbance. High pH of cesium carbonate solutions may also induce ulterior racemization upon incubation. Oligomerization upon modifier excess, paired with digestive deoligomerization, may also gauge CD outcome clarity via the Horeau effect.[145]

Sterics of modification, grain and pore structures

Here we use a combination of computational techniques to model the attempted modifications. Hypothetical structures are built to address potential steric clashes in bulk-modified products. Pore analysis assesses whether bulk modification is accessible via post-synthetic modifier penetration.

In silico modeling: stability of bulk modified products

Uniform appending of incorporated ligands was outlined to be limited by the steric confinement imposed by the framework pores. Building *in silico* models with the modified ligands to address steric clashes may filter out whether desired solid structures already fall through on this criteria. The ligands, modified with both modifications, have been incorporated into both frameworks *in silico*, assuming quantitative modifications. The structure was DFT optimized for UiO-66 NH_2 modified with the (*R*)-**1** aldehyde, further demonstrating that steric clashes do not destabilize the system. It was found that this criterion may not rule out desired uniform bulk modifications. However, observing the apparent hefty pore occupation of the introduced modifications urged the assessment of post-synthetic modifier penetration. Such is necessary, as permitted stability of the end product provides little to support the viability of the experimental route to obtain it.

Pore analysis: bulk modification post-synthetically not accessible

Pore analysis, *in silico*, can reveal whether sterical constraints prohibit incorporation and internal displacement of a guest species within crystalline media. Such is relevant for post-synthetic MOF modification, as contrasting the characteristic modifier radius and the largest free sphere radius within the substrate reflects on the penetration of the former. Surface, shell, or bulk modification patterns may, therefore, become discernible.

To gauge modifier penetration, pore analysis *in silico* was pursued for the flagship system, assessing both modified and unmodified UiO-66 NH_2 substrate. The characteristic lengths of the (*R*)-**1** aldehyde modifying agent were ascertained for its most stable conformer, obtained from DFT optimization (See Supporting Information). The maximum length of the agent in three directions was computed and is 4.604 Å (x direction), 5.656 Å (y direction), and z direction 4.689 Å (Figure 6). Since the agent is not spherical, drawing inspiration from the work of Ongari et al.,[146] we considered drawing an ellipse with its major and minor axes being the plane in which it is studied. For example, if we look into the x direction or yz plane, the ellipse will have its major axis as 5.656 Å and minor axis as 4.689 Å. Given the fact that the pore limiting diameter (Df) of the unmodified and modified substrate is 3.654 Å and 1.387 Å, we can say that even the unmodified substrate cannot fit the said conformer of the chiralizing agent. While dynamic equilibrium of conformers at reaction conditions is assumed, the extent of the misfit renders the results unequivocal.

Findings thus suggest that the obtained modification is predominantly relegated to the grain surface. Even defect-enabled self-limiting shell modification is presumably marginal, if at all relevant, considering how reaction speed may relate to that of Knudsen diffusion.[147]

Experimental results on the extent of relative organic mass incorporation, and on the propensity of the modifier to oligomerize, point to the formation of surface oligomers. Furthermore, given the size range of chiral analytes, the pore analysis's findings translate to steric surface barrier formation in the context of prospective application in enantioseparation. This, in turn, limits diastereomeric interactions to the chiral oligomers on the surface,

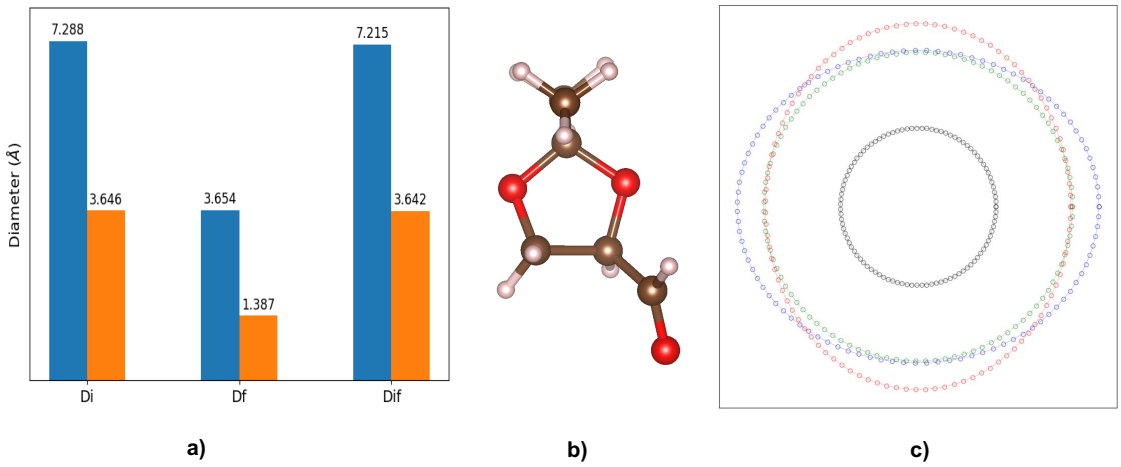

Figure 6: a. Comparison of the pore diameters of the unmodified (blue) and modified (orange) MOF. b. Structure of the most stable conformer of the (*R*)-**1** aldehyde. c. Visualization of the pore aperture of the unmodified MOF (black sphere), and axes of an ellipse encompassing the chiral molecule in different directions: x (blue), y (green), and z (red)

yielding adsorption-based differentiation. In chromatographic separations, diffusion lengths within the stationary phase are highly consequential, as they determine the slope of the van Deemter curve in the ascending régime.[34] Restricting interactions to the surface allows for a favorable separation speed to resolving-power tradeoff, in the parameter threshold relevant for application.

Conclusion

Chiralization of two amine-functionalized MOF substrates was undertaken through treatment with a chiral aldehyde and a chiral ketone. Respective controls with achiral agents were as well performed. Thermogravimetric analyses of relative organic mass have shown instances of incorporation upon these treatments. Elemental analyses have revealed these to be carbon-dominant. As for MIL-125 NH_2, however, solvolythic substrate degradation was pronounced and even prohibitive at harsher reaction conditions. Ligand leaching was observed for MIL-125 NH_2, via the presence of the free chromophore in the reaction solution. Noticeable yield reductions have stressed the extent of solvolythic degradation for this

substrate. PXRD analyses confirmed, however, the retention of the structural backbone in studied solids. In conclusion, compositional analyses revealed a stability–reactivity window, constraining the accessibility of the surveyed chemical space. These findings gauge the scope applicability of this modification method, which is new to MOF chiralization. The UiO-66 NH_2 (*R*)-**1** aldehyde system was, therefore, ascertained to be favorable in this study and became the focus of further inquiry. The use of other chiral oxo compounds for future work is recommended to be limited to aldehydes.

Photographic and infrared spectroscopic analyses of grain surfaces provided direct evidence of covalent modification. Explorative NMR experiments, however, have alluded to a diverse set of resulting species. The HRAM-ESI-MS experiments have detailed the underlying statistical product formation and demonstrated that the target modification is, nevertheless, characteristic. The CD measurements have provided indirect evidence of enantiomeric excess in isolates, showing a retention of enantiomeric excess under process conditions. Target modification was, therefore, concluded to be achieved on the molecular level, with the retention of enantiomeric excess. These findings are consequential as a proof of concept for the feasibility of the novel modification. Furthermore, a detailed description of this chemistry is key for the design of analogous systems.

Computational modeling has revealed that the product yielding from uniform bulk modification of the structure would be sterically stable. In *in silico*, pore analysis has shown the modifier's pore penetration to be marginal, pointing to the dominance of surface modification, nuanced by highly self-limiting pore modification. Distribution of the modification was concluded to be predominantly limited to the surface, forming surface barriers. Reflecting on compositional and molecular-level experimental findings in light of pore analysis, surface modification was concluded to be rich in oligomers. These conclusions suggest the obtained material to be a favorable candidate for use as a stationary phase in chromatographic enantioseparation processes. These findings call for the prospective application of the new material in enentioseparations. Explorative use of the material in a chromatographic setting

is, therefore, suggested for subsequent future work. Furthermore, they serve as a systematic guide for future discovery of similar materials. Present work can also serve as reference material for the study of non-uniform modifications and their radial distribution in MOF.

Conflicts of interest

There are no conflicts of interest to declare.

Acknowledgments

This research was supported by the MARVEL National Centre for Competence in Research, funded by the Swiss National Science Foundation (grant agreement ID 51NF40-182892). The authors acknowledge PRACE and MARVEL for awarding access to Piz Daint (project ID: pr128). The authors thank Dr. Stavroula Kampouri and Dr. Fatmah Mish Ebrahim for providing MOF substrates MIL-125 NH_2 and UiO-66 NH_2 respectively, and Dr. Aisha Asghar for help with photography. The authors thank EPFL facility experts Dr. Aurélien Bornet for dedicated help with NMR experiments, Dr. Roxane Edwige Cécile Moinat for performing elemental analyses, Dr. Laura Piveteau for explorative discussions on MAS-NMR, and Dr. Pascal Alexander Schouwink for training on and maintenance of PXRD instrumentation. Instrument access and training, the laboratory of Prof. Andreas Züttel for TGA, Dr. Luciano Andres Abriata, and the EPFL PTPSP facility for CD is also greatly appreciated.

References

(1) Pasteur, L. Memoires sur la relation qui peut exister entre la forme crystalline et al composition chimique, et sur la cause de la polarization rotatoire. *Compt. rend.* **1848**, *26*, 535–538.

(2) Pasteur, L. Memoire sur la fermentation de l'acide tartrique. *Compt. rend.* **1858**, *46*, 615–618.

(3) Peluso, P.; Chankvetadze, B. Recognition in the domain of molecular chirality: From noncovalent interactions to separation of enantiomers. *Chemical Reviews* **2022**, *122*, 13235–13400.

(4) Fogassy, E.; Faigl, F.; Ács, M. Diastereoisomeric interactions and selective reactions in solutions of enantiomers. *Tetrahedron* **1985**, *41*, 2841–2845.

(5) Hünenberger, P. H.; Granwehr, J. K.; Aebischer, J.-N.; Ghoneim, N.; Haselbach, E.; van Gunsteren, W. F. Experimental and theoretical approach to hydrogen-bonded diastereomeric interactions in a model complex. *Journal of the American Chemical Society* **1997**, *119*, 7533–7544.

(6) Fogassy, E.; Nogradi, M.; Palovics, E.; Schindler, J. Resolution of enantiomers by non-conventional methods. *Synthesis* **2005**, *2005*, 1555–1568.

(7) Habala, L.; Horáková, R.; Čižmáriková, R. Chromatographic separations based on tartaric acid and its derivatives. *Monatshefte für Chemie-Chemical Monthly* **2018**, *149*, 873–882.

(8) Mane, S. Racemic drug resolution: a comprehensive guide. *Analytical Methods* **2016**, *8*, 7567–7586.

(9) Nickerl, G.; Henschel, A.; Grünker, R.; Gedrich, K.; Kaskel, S. Chiral metal-organic

frameworks and their application in asymmetric catalysis and stereoselective separation. *Chemie Ingenieur Technik* **2011**, *83*, 90–103.

(10) Peluso, P.; Mamane, V.; Cossu, S. Homochiral metal–organic frameworks and their application in chromatography enantioseparations. *Journal of Chromatography A* **2014**, *1363*, 11–26.

(11) Duerinck, T.; Denayer, J. Metal-organic frameworks as stationary phases for chiral chromatographic and membrane separations. *Chemical Engineering Science* **2015**, *124*, 179–187.

(12) Bhattacharjee, S.; Khan, M. I.; Li, X.; Zhu, Q.-L.; Wu, X.-T. Recent progress in asymmetric catalysis and chromatographic separation by chiral metal–organic frameworks. *Catalysts* **2018**, *8*, 120.

(13) Liu, J.; Mukherjee, S.; Wang, F.; Fischer, R. A.; Zhang, J. Homochiral metal–organic frameworks for enantioseparation. *Chemical Society Reviews* **2021**, *50*, 5706–5745.

(14) Lu, Y.; Zhang, H.; Zhu, Y.; Marriott, P. J.; Wang, H. Emerging homochiral porous materials for enantiomer separation. *Advanced Functional Materials* **2021**, *31*, 2101335.

(15) Verma, G.; Mehta, R.; Kumar, S.; Ma, S. Metal-Organic Frameworks as a New Platform for Enantioselective Separations. *Israel Journal of Chemistry* **2021**, *61*, 708–726.

(16) Tay, H. M.; Kyratzis, N.; Thoonen, S.; Boer, S. A.; Turner, D. R.; Hua, C. Synthetic strategies towards chiral coordination polymers. *Coordination Chemistry Reviews* **2021**, *435*, 213763.

(17) Siman, P.; Trickett, C. A.; Furukawa, H.; Yaghi, O. M. l-Aspartate links for stable sodium metal–organic frameworks. *Chemical Communications* **2015**, *51*, 17463–17466.

(18) Stylianou, K. C.; Gómez, L.; Imaz, I.; Verdugo-Escamilla, C.; Ribas, X.; Maspoch, D. Engineering homochiral metal–organic frameworks by spatially separating 1D chi-

ral metal–peptide ladders: tuning the pore size for enantioselective adsorption. *Chemistry–A European Journal* **2015**, *21*, 9964–9969.

(19) Zhuo, C.; Wen, Y.; Hu, S.; Sheng, T.; Fu, R.; Xue, Z.; Zhang, H.; Li, H.; Yuan, J.; Chen, X., et al. Homochiral Metal–Organic Frameworks with Tunable Nanoscale Channel Array and Their Enantioseparation Performance against Chiral Diols. *Inorganic Chemistry* **2017**, *56*, 6275–6280.

(20) Lin, L.; Yu, R.; Yang, W.; Wu, X.-Y.; Lu, C.-Z. A series of chiral metal–organic frameworks based on oxalyl retro-peptides: synthesis, characterization, dichroism spectra, and gas adsorption. *Crystal growth & design* **2012**, *12*, 3304–3311.

(21) Grancha, T.; Mon, M.; Ferrando-Soria, J.; Gascon, J.; Seoane, B.; Ramos-Fernandez, E. V.; Armentano, D.; Pardo, E. Tuning the selectivity of light hydrocarbons in natural gas in a family of isoreticular MOFs. *Journal of Materials Chemistry A* **2017**, *5*, 11032–11039.

(22) Mollick, S.; Mukherjee, S.; Kim, D.; Qiao, Z.; Desai, A. V.; Saha, R.; More, Y. D.; Jiang, J.; Lah, M. S.; Ghosh, S. K. Hydrophobic shielding of outer surface: enhancing the chemical stability of metal–organic polyhedra. *Angewandte Chemie* **2019**, *131*, 1053–1057.

(23) Mon, M.; Bruno, R.; Elliani, R.; Tagarelli, A.; Qu, X.; Chen, S.; Ferrando-Soria, J.; Armentano, D.; Pardo, E. Lanthanide discrimination with hydroxyl-decorated flexible metal–organic frameworks. *Inorganic Chemistry* **2018**, *57*, 13895–13900.

(24) Kutzscher, C.; Janssen-Müller, D.; Notzon, A.; Stoeck, U.; Bon, V.; Senkovska, I.; Kaskel, S.; Glorius, F. Synthesis of the homochiral metal–organic framework DUT-129 based on a chiral dicarboxylate linker with 6 stereocenters. *CrystEngComm* **2017**, *19*, 2494–2499.

(25) Cohen, S. M. Postsynthetic methods for the functionalization of metal–organic frameworks. *Chemical reviews* **2012**, *112*, 970–1000.

(26) Cohen, S. M. The postsynthetic renaissance in porous solids. *Journal of the American Chemical Society* **2017**, *139*, 2855–2863.

(27) Burrows, A. D. Mixed-component metal–organic frameworks (MC-MOFs): enhancing functionality through solid solution formation and surface modifications. *CrystEngComm* **2011**, *13*, 3623–3642.

(28) Abd El Sater, M.; Jaber, N.; Schulz, E. Chiral salen complexes for asymmetric heterogeneous catalysis: Recent examples for recycling and cooperativity. *ChemCatChem* **2019**, *11*, 3662–3687.

(29) Freire, C.; Nunes, M.; Pereira, C.; Fernandes, D. M.; Peixoto, A. F.; Rocha, M. Metallo (salen) complexes as versatile building blocks for the fabrication of molecular materials and devices with tuned properties. *Coordination Chemistry Reviews* **2019**, *394*, 104–134.

(30) Yuan, G.; Jiang, H.; Zhang, L.; Liu, Y.; Cui, Y. Metallosalen-based crystalline porous materials: Synthesis and property. *Coordination Chemistry Reviews* **2019**, *378*, 483–499.

(31) Yin, Z.; Wan, S.; Yang, J.; Kurmoo, M.; Zeng, M.-H. Recent advances in post-synthetic modification of metal–organic frameworks: New types and tandem reactions. *Coordination Chemistry Reviews* **2019**, *378*, 500–512.

(32) Kaur, M.; Kumar, S.; Yusuf, M.; Lee, J.; Brown, R. J.; Kim, K.-H.; Malik, A. K. Post-synthetic modification of luminescent metal-organic frameworks using schiff base complexes for biological and chemical sensing. *Coordination Chemistry Reviews* **2021**, *449*, 214214.

(33) Jablonka, K. M.; Moosavi, S. M.; Asgari, M.; Ireland, C.; Patiny, L.; Smit, B. A data-driven perspective on the colours of metal–organic frameworks. *Chemical science* **2021**, *12*, 3587–3598.

(34) Catani, M.; Ismail, O. H.; Gasparrini, F.; Antonelli, M.; Pasti, L.; Marchetti, N.; Felletti, S.; Cavazzini, A. Recent advancements and future directions of superficially porous chiral stationary phases for ultrafast high-performance enantioseparations. *Analyst* **2017**, *142*, 555–566.

(35) Prout, C.; Carruthers, J.; Rossotti, F. Structure and stability of carboxylate complexes. Part VII. Crystal and molecular structures of copper (II) meso-tartrate trihydrate and copper (II) d-tartrate trihydrate. *Journal of the Chemical Society A: Inorganic, Physical, Theoretical* **1971**, 3336–3342.

(36) Bostelaar, L. J.; De Graaff, R. A.; Hulsbergen, F. B.; Reedijk, J.; Sachtler, W. M. Synthesis, structure, and spectral characterization of nickel (II)(R, R)-tartrate. Crystal and molecular structure of polymeric diaquabis ((R, R)-tartrato-O1, O2: O3, O4) dinickel (II) trihydrate at-162. degree. C. *Inorganic Chemistry* **1984**, *23*, 2294–2297.

(37) Bagi, P.; Ujj, V.; Czugler, M.; Fogassy, E.; Keglevich, G. Resolution of P-stereogenic P-heterocycles via the formation of diastereomeric molecular and coordination complexes (a review). *Dalton Transactions* **2016**, *45*, 1823–1842.

(38) Gu, Z.-G.; Zhan, C.; Zhang, J.; Bu, X. Chiral chemistry of metal–camphorate frameworks. *Chemical Society Reviews* **2016**, *45*, 3122–3144.

(39) Imaz, I.; Rubio-Martinez, M.; An, J.; Sole-Font, I.; Rosi, N. L.; Maspoch, D. Metal–biomolecule frameworks (MBioFs). *Chemical communications* **2011**, *47*, 7287–7302.

(40) Anderson, S. L.; Stylianou, K. C. Biologically derived metal organic frameworks. *Coordination Chemistry Reviews* **2017**, *349*, 102–128.

(41) Cai, H.; Huang, Y.-L.; Li, D. Biological metal–organic frameworks: Structures, host–guest chemistry and bio-applications. *Coordination Chemistry Reviews* **2019**, *378*, 207–221.

(42) He, Y.; Hou, X.; Liu, Y.; Feng, N. Recent progress in the synthesis, structural diversity and emerging applications of cyclodextrin-based metal–organic frameworks. *Journal of Materials Chemistry B* **2019**, *7*, 5602–5619.

(43) Rajkumar, T.; Kukkar, D.; Kim, K.-H.; Sohn, J. R.; Deep, A. Cyclodextrin-metal–organic framework (CD-MOF): From synthesis to applications. *Journal of Industrial and Engineering Chemistry* **2019**, *72*, 50–66.

(44) Nadar, S. S.; Vaidya, L.; Maurya, S.; Rathod, V. K. Polysaccharide based metal organic frameworks (polysaccharide–MOF): A review. *Coordination Chemistry Reviews* **2019**, *396*, 1–21.

(45) Roy, I.; Stoddart, J. F. Cyclodextrin metal–organic frameworks and their applications. *Accounts of chemical research* **2021**, *54*, 1440–1453.

(46) Zhang, H.; Zou, R.; Zhao, Y. Macrocycle-based metal-organic frameworks. *Coordination Chemistry Reviews* **2015**, *292*, 74–90.

(47) Valente, C.; Choi, E.; Belowich, M. E.; Doonan, C. J.; Li, Q.; Gasa, T. B.; Botros, Y. Y.; Yaghi, O. M.; Stoddart, J. F. Metal–organic frameworks with designed chiral recognition sites. *Chemical communications* **2010**, *46*, 4911–4913.

(48) Li, Q.; Zhang, W.; Miljanić, O. Š.; Sue, C.-H.; Zhao, Y.-L.; Liu, L.; Knobler, C. B.; Stoddart, J. F.; Yaghi, O. M. Docking in metal-organic frameworks. *Science* **2009**, *325*, 855–859.

(49) Yoon, M.; Srirambalaji, R.; Kim, K. Homochiral metal–organic frameworks for asymmetric heterogeneous catalysis. *Chemical reviews* **2012**, *112*, 1196–1231.

(50) Falkowski, J. M.; Liu, S.; Lin, W. Metal-Organic Frameworks as Single-Site Solid Catalysts for Asymmetric Reactions. *Israel Journal of Chemistry* **2012**, *52*, 591–603.

(51) Sharifzadeh, Z.; Berijani, K.; Morsali, A. Chiral metal–organic frameworks based on asymmetric synthetic strategies and applications. *Coordination Chemistry Reviews* **2021**, *445*, 214083.

(52) Pschirer, N. G.; Ciurtin, D. M.; Smith, M. D.; Bunz, U. H.; zur Loye, H.-C. Noninterpenetrating Square-Grid Coordination Polymers With Dimensions of 25× 25 Å2 Prepared by Using N, N'-Type Ligands: The First Chiral Square-Grid Coordination Polymer. *Angewandte Chemie International Edition* **2002**, *41*, 583–585.

(53) Hawes, C. S.; Fitchett, C. M.; Batten, S. R.; Kruger, P. E. Synthesis and structural characterisation of a Co (II) coordination polymer incorporating a novel dicarboxy-Trögers base/bis-pyrazole mixed ligand system. *Inorganica Chimica Acta* **2012**, *389*, 112–117.

(54) Robin, J.; Audebrand, N.; Poriel, C.; Canivet, J.; Calvez, G.; Roisnel, T.; Dorcet, V.; Roussel, P. A series of chiral metal–organic frameworks based on fluorene di-and tetracarboxylates: syntheses, crystal structures and luminescence properties. *CrystEngComm* **2017**, *19*, 2042–2056.

(55) Jablonka, K. M.; Ongari, D.; Moosavi, S. M.; Smit, B. Big-data science in porous materials: materials genomics and machine learning. *Chemical reviews* **2020**, *120*, 8066–8129.

(56) Majumdar, S.; Moosavi, S. M.; Jablonka, K. M.; Ongari, D.; Smit, B. Diversifying databases of metal organic frameworks for high-throughput computational screening. *ACS applied materials & interfaces* **2021**, *13*, 61004–61014.

(57) Zunger, A. Inverse design in search of materials with target functionalities. *Nature Reviews Chemistry* **2018**, *2*, 1–16.

(58) Noh, J.; Gu, G. H.; Kim, S.; Jung, Y. Machine-enabled inverse design of inorganic solid materials: promises and challenges. *Chemical Science* **2020**, *11*, 4871–4881.

(59) Pollice, R.; dos Passos Gomes, G.; Aldeghi, M.; Hickman, R. J.; Krenn, M.; Lavigne, C.; Lindner-D'Addario, M.; Nigam, A.; Ser, C. T.; Yao, Z., et al. Data-driven strategies for accelerated materials design. *Accounts of Chemical Research* **2021**, *54*, 849–860.

(60) Bao, X.; Broadbelt, L. J.; Snurr, R. Q. A computational study of enantioselective adsorption in a homochiral metal–organic framework. *Molecular Simulation* **2009**, *35*, 50–59.

(61) Bao, X.; Broadbelt, L. J.; Snurr, R. Q. Computational screening of homochiral metal–organic frameworks for enantioselective adsorption. *Microporous and mesoporous materials* **2012**, *157*, 118–123.

(62) Moghadam, P. Z.; Düren, T. Origin of enantioselectivity in a chiral metal–organic framework: a molecular simulation study. *The Journal of Physical Chemistry C* **2012**, *116*, 20874–20881.

(63) Qiao, Z.; Torres-Knoop, A.; Dubbeldam, D.; Fairen-Jimenez, D.; Zhou, J.; Snurr, R. Q. Advanced Monte Carlo simulations of the adsorption of chiral alcohols in a homochiral metal-organic framework. *AIChE Journal* **2014**, *60*, 2324–2334.

(64) Todorova, T. K.; Rozanska, X.; Gervais, C.; Legrand, A.; Ho, L. N.; Berruyer, P.; Lesage, A.; Emsley, L.; Farrusseng, D.; Canivet, J., et al. Molecular Level Characterization of the Structure and Interactions in Peptide-Functionalized Metal–Organic Frameworks. *Chemistry–A European Journal* **2016**, *22*, 16531–16538.

(65) Canivet, J.; Bernoud, E.; Bonnefoy, J.; Legrand, A.; Todorova, T. K.; Quadrelli, E. A.; Mellot-Draznieks, C. Synthetic and computational assessment of a chiral metal–

organic framework catalyst for predictive asymmetric transformation. *Chemical science* **2020**, *11*, 8800–8808.

(66) Qiao, Z.; Li, L.; Li, S.; Liang, H.; Zhou, J.; Snurr, R. Q. Molecular fingerprint and machine learning to accelerate design of high-performance homochiral metal–organic frameworks. *AIChE Journal* **2021**, *67*, e17352.

(67) Bunck, D. N.; Dichtel, W. R. Mixed linker strategies for organic framework functionalization. *Chemistry–A European Journal* **2013**, *19*, 818–827.

(68) Lun, D. J.; Waterhouse, G. I.; Telfer, S. G. A general thermolabile protecting group strategy for organocatalytic metal- organic frameworks. *Journal of the American Chemical Society* **2011**, *133*, 5806–5809.

(69) Kutzscher, C.; Nickerl, G.; Senkovska, I.; Bon, V.; Kaskel, S. Proline functionalized UiO-67 and UiO-68 type metal–organic frameworks showing reversed diastereoselectivity in aldol addition reactions. *Chemistry of Materials* **2016**, *28*, 2573–2580.

(70) Sawano, T.; Ji, P.; McIsaac, A. R.; Lin, Z.; Abney, C. W.; Lin, W. The first chiral diene-based metal–organic frameworks for highly enantioselective carbon–carbon bond formation reactions. *Chemical science* **2015**, *6*, 7163–7168.

(71) Kiang, Y.-H.; Gardner, G. B.; Lee, S.; Xu, Z.; Lobkovsky, E. B. Variable pore size, variable chemical functionality, and an example of reactivity within porous phenylacetylene silver salts. *Journal of the American Chemical Society* **1999**, *121*, 8204–8215.

(72) Newar, R.; Akhtar, N.; Antil, N.; Kumar, A.; Shukla, S.; Begum, W.; Manna, K. Amino Acid-Functionalized Metal-Organic Frameworks for Asymmetric Base–Metal Catalysis. *Angewandte Chemie International Edition* **2021**, *60*, 10964–10970.

(73) Zhang, Y.; Gui, B.; Chen, R.; Hu, G.; Meng, Y.; Yuan, D.; Zeller, M.; Wang, C. Engineering a zirconium MOF through tandem "click" reactions: a general strategy for quantitative loading of bifunctional groups on the pore surface. *Inorganic Chemistry* **2018**, *57*, 2288–2295.

(74) Liu, T.-Y.; Qu, X.-L.; Yan, B. A sensitive metal–organic framework nanosensor with cation-introduced chirality for enantioselective recognition and determination of quinine and quinidine in human urine. *Journal of Materials Chemistry C* **2020**, *8*, 14579–14586.

(75) Cao, L.-H.; Shi, F.; Zhang, W.-M.; Zang, S.-Q.; Mak, T. C. Selective Sensing of Fe3+ and Al3+ Ions and Detection of 2, 4, 6-Trinitrophenol by a Water-Stable Terbium-Based Metal–Organic Framework. *Chemistry–A European Journal* **2015**, *21*, 15705–15712.

(76) Cao, L.-H.; Li, H.-Y.; Xu, H.; Wei, Y.-L.; Zang, S.-Q. Diverse dissolution–recrystallization structural transformations and sequential Förster resonance energy transfer behavior of a luminescent porous Cd-MOF. *Dalton Transactions* **2017**, *46*, 11656–11663.

(77) Nießing, S.; Czekelius, C.; Janiak, C. Immobilisation of catalytically active proline on H2N-MIL-101 (Al) accompanied with reversal in enantioselectivity. *Catalysis Communications* **2017**, *95*, 12–15.

(78) Gedrich, K.; Heitbaum, M.; Notzon, A.; Senkovska, I.; Fröhlich, R.; Getzschmann, J.; Mueller, U.; Glorius, F.; Kaskel, S. A family of chiral metal–organic frameworks. *Chemistry–A European Journal* **2011**, *17*, 2099–2106.

(79) Padmanaban, M.; Müller, P.; Lieder, C.; Gedrich, K.; Grünker, R.; Bon, V.; Senkovska, I.; Baumgärtner, S.; Opelt, S.; Paasch, S., et al. Application of a chiral

metal–organic framework in enantioselective separation. *Chemical Communications* **2011**, *47*, 12089–12091.

(80) Wu, P.; He, C.; Wang, J.; Peng, X.; Li, X.; An, Y.; Duan, C. Photoactive chiral metal–organic frameworks for light-driven asymmetric α-alkylation of aldehydes. *Journal of the American Chemical Society* **2012**, *134*, 14991–14999.

(81) Han, Q.; He, C.; Zhao, M.; Qi, B.; Niu, J.; Duan, C. Engineering chiral polyoxometalate hybrid metal–organic frameworks for asymmetric dihydroxylation of olefins. *Journal of the American Chemical Society* **2013**, *135*, 10186–10189.

(82) Cheng, L.; Zhao, K.; Zhang, Q.; Li, Y.; Zhai, Q.; Chen, J.; Lou, Y. Chiral Proline-Decorated Bifunctional Pd@ NH2-UiO-66 Catalysts for Efficient Sequential Suzuki Coupling/Asymmetric Aldol Reactions. *Inorganic Chemistry* **2020**, *59*, 7991–8001.

(83) Canivet, J.; Aguado, S.; Bergeret, G.; Farrusseng, D. Amino acid functionalized metal–organic frameworks by a soft coupling–deprotection sequence. *Chemical Communications* **2011**, *47*, 11650–11652.

(84) Bonnefoy, J.; Legrand, A.; Quadrelli, E. A.; Canivet, J.; Farrusseng, D. Enantiopure peptide-functionalized metal–organic frameworks. *Journal of the American Chemical Society* **2015**, *137*, 9409–9416.

(85) Canivet, J.; Farrusseng, D. Proline-functionalized metal–organic frameworks and their use in asymmetric catalysis: pitfalls in the MOFs rush. *RSC Advances* **2015**, *5*, 11254–11256.

(86) Kou, W.-T.; Yang, C.-X.; Yan, X.-P. Post-synthetic modification of metal–organic frameworks for chiral gas chromatography. *Journal of Materials Chemistry A* **2018**, *6*, 17861–17866.

(87) Lu, Y.; Zhang, H.; Chan, J. Y.; Ou, R.; Zhu, H.; Forsyth, M.; Marijanovic, E. M.; Doherty, C. M.; Marriott, P. J.; Holl, M. M. B., et al. Homochiral MOF–polymer mixed matrix membranes for efficient separation of chiral molecules. *Angewandte Chemie* **2019**, *131*, 17084–17091.

(88) Lin, C.; He, H.; Zhang, Y.; Xu, M.; Tian, F.; Li, L.; Wang, Y. Acetaldehyde-modified-cystine functionalized Zr-MOFs for pH/GSH dual-responsive drug delivery and selective visualization of GSH in living cells. *RSC advances* **2020**, *10*, 3084–3091.

(89) Zhou, S.; Guo, J.; Dai, Z.; Liu, C.; Zhao, J.; Gao, Z.; Song, Y.-Y. Engineering homochiral MOFs in TiO2 nanotubes as enantioselective photoelectrochemical electrode for chiral recognition. *Analytical Chemistry* **2021**, *93*, 12067–12074.

(90) Garibay, S. J.; Wang, Z.; Tanabe, K. K.; Cohen, S. M. Postsynthetic modification: a versatile approach toward multifunctional metal-organic frameworks. *Inorganic chemistry* **2009**, *48*, 7341–7349.

(91) Yang, X.-L.; Zang, R.-B.; Shao, R.; Guan, R.-F.; Xie, M.-H. Chiral UiO-MOFs based QCM sensors for enantioselective discrimination of hazardous biomolecule. *Journal of Hazardous Materials* **2021**, *413*, 125467.

(92) Cao, Q.; Peng, Y.; Yu, Q.; Shi, Z.; Jia, Q. Post synthetic modification of Zr-MOF with phenylboronic acid: Fluorescence sensing of sialic acid. *Dyes and Pigments* **2022**, *197*, 109839.

(93) Zhu, W.; He, C.; Wu, P.; Wu, X.; Duan, C. "Click" post-synthetic modification of metal–organic frameworks with chiral functional adduct for heterogeneous asymmetric catalysis. *Dalton Transactions* **2012**, *41*, 3072–3077.

(94) Nguyen, K. D.; Kutzscher, C.; Drache, F.; Senkovska, I.; Kaskel, S. Chiral functionalization of a zirconium metal–organic framework (DUT-67) as a heterogeneous catalyst in asymmetric Michael addition reaction. *Inorganic Chemistry* **2018**, *57*, 1483–1489.

(95) Rani, R.; Deep, A.; Mizaikoff, B.; Singh, S. Enhanced hydrothermal stability of Cu MOF by post synthetic modification with amino acids. *Vacuum* **2019**, *164*, 449–457.

(96) Ahmed, I.; Yunus, U.; Nadeem, M.; Bhatti, M. H.; Mehmood, M. Post synthetically modified compounds of Cd-MOF by l-amino acids for luminescent applications. *Journal of Solid State Chemistry* **2020**, *287*, 121320.

(97) Ma, X.; Guo, Y.; Zhang, L.; Wang, K.; Yu, A.; Zhang, S.; Ouyang, G. Crystal morphology tuning and green post-synthetic modification of metal organic framework for HPLC enantioseparation. *Talanta* **2022**, *239*, 123143.

(98) Ullah, S.; Yunus, U.; Bhatti, M. H.; Southon, P. D.; Iqbal, K.; Zaidi, S. Homochiral Metal Organic Frameworks and Their Usage for the Enantio-Purification of Racemic Drugs. *ChemistrySelect* **2018**, *3*, 10434–10438.

(99) Gheorghe, A.; Strudwick, B.; Dawson, D. M.; Ashbrook, S. E.; Woutersen, S.; Dubbeldam, D.; Tanase, S. Synthesis of Chiral MOF-74 Frameworks by Post-Synthetic Modification by Using an Amino Acid. *Chemistry–A European Journal* **2020**, *26*, 13957–13965.

(100) Hu, X.-J.; Huang, G.; Zhang, S.; Fang, Z.-B.; Liu, T.-F.; Cao, R. An easy and low-cost method of embedding chiral molecules in metal–organic frameworks for enantioseparation. *Chemical Communications* **2020**, *56*, 7459–7462.

(101) Berijani, K.; Morsali, A. Dual activity of durable chiral hydroxyl-rich MOF for asymmetric catalytic reactions. *Journal of Catalysis* **2019**, *378*, 28–35.

(102) Berijani, K.; Morsali, A.; Hupp, J. T. An effective strategy for creating asymmetric MOFs for chirality induction: a chiral Zr-based MOF for enantioselective epoxidation. *Catalysis Science & Technology* **2019**, *9*, 3388–3397.

(103) Banerjee, M.; Das, S.; Yoon, M.; Choi, H. J.; Hyun, M. H.; Park, S. M.; Seo, G.; Kim, K. Postsynthetic modification switches an achiral framework to catalytically active homochiral metal- organic porous materials. *Journal of the American Chemical Society* **2009**, *131*, 7524–7525.

(104) Shi, T.; Guo, Z.; Yu, H.; Xie, J.; Zhong, Y.; Zhu, W. Atom-economic synthesis of optically active Warfarin anticoagulant over a chiral MOF organocatalyst. *Advanced Synthesis & Catalysis* **2013**, *355*, 2538–2543.

(105) Xi, W.; Liu, Y.; Xia, Q.; Li, Z.; Cui, Y. Direct and Post-Synthesis Incorporation of Chiral Metallosalen Catalysts into Metal–Organic Frameworks for Asymmetric Organic Transformations. *Chemistry–A European Journal* **2015**, *21*, 12581–12585.

(106) Tan, C.; Han, X.; Li, Z.; Liu, Y.; Cui, Y. Controlled exchange of achiral linkers with chiral linkers in Zr-based UiO-68 metal–organic framework. *Journal of the American Chemical Society* **2018**, *140*, 16229–16236.

(107) Chen, D.; Luo, R.; Li, M.; Wen, M.; Li, Y.; Chen, C.; Zhang, N. Salen (Co (iii)) imprisoned within pores of a metal–organic framework by post-synthetic modification and its asymmetric catalysis for CO 2 fixation at room temperature. *Chemical Communications* **2017**, *53*, 10930–10933.

(108) Roy, P.; Schaate, A.; Behrens, P.; Godt, A. Post-Synthetic Modification of Zr-Metal–Organic Frameworks through Cycloaddition Reactions. *Chemistry–A European Journal* **2012**, *18*, 6979–6985.

(109) Hindelang, K.; Vagin, S. I.; Anger, C.; Rieger, B. Tandem post-synthetic modification for functionalized metal–organic frameworks via epoxidation and subsequent epoxide ring-opening. *Chemical Communications* **2012**, *48*, 2888–2890.

(110) Karmakar, A.; Hazra, S.; Pombeiro, A. J. Urea and thiourea based coordination poly-

mers and metal-organic frameworks: Synthesis, structure and applications. *Coordination Chemistry Reviews* **2021**, 214314.

(111) Volkringer, C.; Cohen, S. M. Generating reactive MILs: isocyanate-and isothiocyanate-bearing MILs through postsynthetic modification. *Angewandte Chemie* **2010**, *122*, 4748–4752.

(112) Saleem, H.; Rafique, U.; Davies, R. P. Investigations on post-synthetically modified UiO-66-NH2 for the adsorptive removal of heavy metal ions from aqueous solution. *Microporous and Mesoporous Materials* **2016**, *221*, 238–244.

(113) Li, W.-Y.; Yang, S.; Li, Y.-A.; Li, Q.-Y.; Guan, Q.; Dong, Y.-B. Synthesis of an MOF-based Hg 2+-fluorescent probe via stepwise post-synthetic modification in a single-crystal-to-single-crystal fashion and its application in bioimaging. *Dalton Transactions* **2019**, *48*, 16502–16508.

(114) Dugan, E.; Wang, Z.; Okamura, M.; Medina, A.; Cohen, S. M. Covalent modification of a metal–organic framework with isocyanates: probing substrate scope and reactivity. *Chemical communications* **2008**, 3366–3368.

(115) Bernt, S.; Guillerm, V.; Serre, C.; Stock, N. Direct covalent post-synthetic chemical modification of Cr-MIL-101 using nitrating acid. *Chemical communications* **2011**, *47*, 2838–2840.

(116) Dong, X.-W.; Liu, T.; Hu, Y.-Z.; Liu, X.-Y.; Che, C.-M. Urea postmodified in a metal–organic framework as a catalytically active hydrogen-bond-donating heterogeneous catalyst. *Chemical Communications* **2013**, *49*, 7681–7683.

(117) Luan, Y.; Zheng, N.; Qi, Y.; Tang, J.; Wang, G. Merging metal–organic framework catalysis with organocatalysis: A thiourea functionalized heterogeneous catalyst at the nanoscale. *Catalysis Science & Technology* **2014**, *4*, 925–929.

(118) Burrows, A. D.; Frost, C. G.; Mahon, M. F.; Richardson, C. Post-Synthetic Modification of Tagged Metal–Organic Frameworks. *Angewandte Chemie* **2008**, *120*, 8610–8614.

(119) Morris, W.; Doonan, C. J.; Furukawa, H.; Banerjee, R.; Yaghi, O. M. Crystals as molecules: postsynthesis covalent functionalization of zeolitic imidazolate frameworks. *Journal of the American Chemical Society* **2008**, *130*, 12626–12627.

(120) Ingleson, M. J.; Barrio, J. P.; Guilbaud, J.-B.; Khimyak, Y. Z.; Rosseinsky, M. J. Framework functionalisation triggers metal complex binding. *Chemical Communications* **2008**, 2680–2682.

(121) Kaposi, M.; Cokoja, M.; Hutterer, C. H.; Hauser, S. A.; Kaposi, T.; Klappenberger, F.; Pöthig, A.; Barth, J. V.; Herrmann, W. A.; Kühn, F. E. Immobilisation of a molecular epoxidation catalyst on UiO-66 and-67: the effect of pore size on catalyst activity and recycling. *Dalton Transactions* **2015**, *44*, 15976–15983.

(122) Liu, L.; Tai, X.; Zhou, X.; Liu, L. Synthesis, post-modification and catalytic properties of metal-organic framework NH2-MIL-53 (Al). *Chemical Research in Chinese Universities* **2017**, *33*, 231–238.

(123) Daliran, S.; Santiago-Portillo, A.; Navalón, S.; Oveisi, A. R.; Álvaro, M.; Ghorbani-Vaghei, R.; Azarifar, D.; García, H. Cu (II)-Schiff base covalently anchored to MIL-125 (Ti)-NH2 as heterogeneous catalyst for oxidation reactions. *Journal of colloid and interface science* **2018**, *532*, 700–710.

(124) Zhu, S.-Y.; Yan, B. A novel covalent post-synthetically modified MOF hybrid as a sensitive and selective fluorescent probe for Al 3+ detection in aqueous media. *Dalton Transactions* **2018**, *47*, 1674–1681.

(125) Wu, X.; Lin, J.; Xie, J.; Zhao, X.; Liu, D.; Xing, Y.; Xu, L. Salen–Mg-doped NH2–MIL-

101 (Cr) for effective CO2 adsorption under ambient conditions. *Applied Organometallic Chemistry* **2020**, *34*, e5993.

(126) Hossain, S.; Jalil, M. A Recyclable Heterogeneous Palladium Catalyst Anchored to Modified Metal-Organic Framework for Hydrogenation of Styrene Oxide. *Russian Journal of Organic Chemistry* **2019**, *55*, 1946–1950.

(127) Qin, Y.; Wang, B.; Li, J.; Wu, X.; Chen, L. Cobalt imine–pyridine–carbonyl complex functionalized metal–organic frameworks as catalysts for alkene epoxidation. *Transition Metal Chemistry* **2019**, *44*, 595–602.

(128) Zhu, S.-Y.; Yan, B. Highly sensitive luminescent probe of aniline and trace water in organic solvents based on covalently modified lanthanide metal–organic frameworks. *Industrial & Engineering Chemistry Research* **2018**, *57*, 16564–16571.

(129) Zhu, S.-Y.; Yan, B. A novel sensitive fluorescent probe of S 2 O 8 2- and Fe 3+ based on covalent post-functionalization of a zirconium (iv) metal–organic framework. *Dalton Transactions* **2018**, *47*, 11586–11592.

(130) Qu, S.; Cao, Q.; Ma, J.; Jia, Q. A turn-on fluorescence sensor for creatinine based on the quinoline-modified metal organic frameworks. *Talanta* **2020**, *219*, 121280.

(131) Dalapati, R.; Biswas, S. Post-synthetic modification of a metal-organic framework with fluorescent-tag for dual naked-eye sensing in aqueous medium. *Sensors and Actuators B: Chemical* **2017**, *239*, 759–767.

(132) Du, Y.; Li, X.; Lv, X.; Jia, Q. Highly sensitive and selective sensing of free bilirubin using metal–organic frameworks-based energy transfer process. *ACS applied materials & interfaces* **2017**, *9*, 30925–30932.

(133) Wang, J.; Xia, T.; Zhang, X.; Zhang, Q.; Cui, Y.; Yang, Y.; Qian, G. A turn-on fluorescent probe for Cd 2+ detection in aqueous environments based on an imine

functionalized nanoscale metal–organic framework. *RSC advances* **2017**, *7*, 54892–54897.

(134) Bhattacharjee, S.; Yang, D.-A.; Ahn, W.-S. A new heterogeneous catalyst for epoxidation of alkenes via one-step post-functionalization of IRMOF-3 with a manganese (II) acetylacetonate complex. *Chemical Communications* **2011**, *47*, 3637–3639.

(135) Lin, Y.; Kong, C.; Chen, L. Amine-functionalized metal–organic frameworks: structure, synthesis and applications. *RSC advances* **2016**, *6*, 32598–32614.

(136) Yoo, D. K.; Ahmed, I.; Sarker, M.; Lee, H. J.; Vinu, A.; Jhung, S. H. Metal–organic frameworks containing uncoordinated nitrogen: Preparation, modification, and application in adsorption. *Materials Today* **2021**,

(137) Fu, Y.; Sun, D.; Chen, Y.; Huang, R.; Ding, Z.; Fu, X.; Li, Z. An amine-functionalized titanium metal–organic framework photocatalyst with visible-light-induced activity for CO2 reduction. *Angewandte Chemie International Edition* **2012**, *51*, 3364–3367.

(138) Vermoortele, F.; Ameloot, R.; Vimont, A.; Serre, C.; De Vos, D. An amino-modified Zr-terephthalate metal–organic framework as an acid–base catalyst for cross-aldol condensation. *Chemical communications* **2011**, *47*, 1521–1523.

(139) Schmid, C. R.; Bryant, J. D.; Dowlatzedah, M.; Phillips, J. L.; Prather, D. E.; Schantz, R. D.; Sear, N. L.; Vianco, C. S. Synthesis of 2, 3-O-isopropylidene-D-glyceraldehyde in high chemical and optical purity: observations on the development of a practical bulk process. *The journal of organic chemistry* **1991**, *56*, 4056–4058.

(140) de O. Domingos, J. L.; de A. Vilela, G. V.; Costa, P. R.; Dias, A. G. Crude D-(+)-Glyceraldehyde Obtained from D-Mannitol-Diacetonide by Oxidative Cleavage with Sodium Periodate: Its Reactions with Nucleophilic Species. *Synthetic communications* **2004**, *34*, 589–598.

(141) Kampouri, S.; Ebrahim, F. M.; Fumanal, M.; Nord, M.; Schouwink, P. A.; Elzein, R.; Addou, R.; Herman, G. S.; Smit, B.; Ireland, C. P., et al. Enhanced visible-light-driven hydrogen production through MOF/MOF heterojunctions. *ACS Applied Materials & Interfaces* **2021**, *13*, 14239–14247.

(142) Garibay, S. J.; Cohen, S. M. Isoreticular synthesis and modification of frameworks with the UiO-66 topology. *Chemical communications* **2010**, *46*, 7700–7702.

(143) Chu, J.; Ke, F.-S.; Wang, Y.; Feng, X.; Chen, W.; Ai, X.; Yang, H.; Cao, Y. Facile and reversible digestion and regeneration of zirconium-based metal-organic frameworks. *Communications Chemistry* **2020**, *3*, 5.

(144) Christensen, J. J.; Eatough, D. J.; Izatt, R. M. The synthesis and ion bindings of synthetic multidentate macrocyclic compounds. *Chemical reviews* **1974**, *74*, 351–384.

(145) Horeau, A. Interactions d'enantiomeres en solution; influence sur le pouvoir rotatoire: Purete optique et purete enantiomerique. *Tetrahedron Letters* **1969**, *10*, 3121–3124.

(146) Ongari, D.; Liu, Y. M.; Smit, B. Can Metal–Organic Frameworks Be Used for Cannabis Breathalyzers? *ACS applied materials & interfaces* **2019**, *11*, 34777–34786.

(147) Gao, W.-Y.; Cardenal, A. D.; Wang, C.-H.; Powers, D. C. In Operando Analysis of Diffusion in Porous Metal-Organic Framework Catalysts. *Chemistry–A European Journal* **2019**, *25*, 3465–3476.